Journal for ImmunoTherapy of Cancer

Tryptophan potentiates CD8+ T cells against cancer cells by TRIP12 tryptophanylation and surface PD-1 downregulation

Rui Qin,[1] Chen Zhao,[1] Chen-Ji Wang,[1] Wei Xu,[2,3] Jian-Yuan Zhao,[2,3] Yan Lin,[2,3] Yi-Yuan Yuan,[2,3] Peng-Cheng Lin,[4] Yao Li,[1] Shimin Zhao ,[1,2] Yan Huang[1]

For numbered affiliations see end of article.

Correspondence to
Dr Shimin Zhao;
zhaosm@fudan.edu.cn

Dr Yao Li; yaoli@fudan.edu.cn

Dr Yan Huang;
huangyan@fudan.edu.cn

ABSTRACT

Background Tryptophan catabolites suppress immunity. Therefore, blocking tryptophan catabolism with indoleamine 2,3-dioxygenase (IDO) inhibitors is pursued as an anticancer strategy.

Methods The intracellular level of tryptophan and kynurenine was detected by mass spectrum analysis. The effect of tryptophan and IDO inhibitors on cell surface programmed cell death protein 1 (PD-1) level were measured by flow cytometry. A set of biochemical analyses were used to figure out the underlying mechanism. In vitro co-culture system, syngeneic mouse models, immunofluorescent staining, and flow cytometry analysis were employed to investigate the role of tryptophan and IDO inhibitor in regulating the cytotoxicity of CD8+ T cells.

Results Here, we reported that IDO inhibitors activated CD8+ T cells also by accumulating tryptophan that downregulated PD-1. Tryptophan and IDO inhibitors administration, both increased intracellular tryptophan, and tryptophanyl-tRNA synthetase (WARS) overexpression decreased Jurkat and mice CD8+ T cell surface PD-1. Mechanistically, WARS tryptophanylated lysine 1136 of and activated E3 ligase TRIP12 to degrade NFATc1, a PD-1 transcription activator. SIRT1 de-tryptophanylated TRIP12 and reversed the effects of tryptophan and WARS on PD-1. Tryptophan or IDO inhibitors potentiated CD8+ T cells to induce apoptosis of co-cultured cancer cells, increased cancer-infiltrating CD8+ T cells and slowed down tumor growth of lung cancer in mice.

Conclusions Our results revealed the immune-activating efficacy of tryptophan, and suggested tryptophan supplemental may benefit IDO inhibitors and PD-1 blockade during anticancer treatments.

INTRODUCTION

Cancer cells express programmed death ligand 1 (PD-L1) on their surface and use it to interact with the T cell programmed cell death protein 1 (PD-1), a major regulator of T cell exhaustion that leads to the loss of T cell proliferative capacity and CD8+ T effector function,[1 2] to escape an immune attack.[3] Cancer immune therapy aims to either boost the body's natural immune defense or decrease immune escape of cancer cells.

Eliminating PD-L1 prevents immune escape of cancer cells. Blocking the PD-1 pathway restores T cell function and improves tumor eradication.[4] Therefore, inhibitors of both PD-L1 and PD-1 are clinically used as drugs to treat cancers, such as melanoma, advanced lung cancer, kidney cancer, bladder cancer, and Hodgkin's lymphoma.[3]

Tryptophan is an essential amino acid whose catabolism is extensively studied in cancer biology because of its close association with cancer and immune responses. The major tryptophan-catabolizing enzyme indoleamine-2,3-dioxygenase (IDO)[5] is overexpressed in such cancers as gastric, colon, and renal cell carcinomas,[6] tryptophan catabolism is critical for maintaining the immune privilege of the placenta,[7] and blocking IDO with IDO inhibitors, such as l-isomer of methylated tryptophan (L-1-MT), showed anticancer effects in preclinical models.[5 8 9] As the rate-limiting enzyme, IDO converts >95% tryptophan into kynurenine.[10 11] Moreover, downstream metabolites of tryptophan catabolism, such as kynurenine, act to suppress certain immune cells, probably via pro-apoptotic mechanisms.[12] Thus, theories have been postulated to suggest that tryptophan catabolism is necessary for maintaining certain aspects of immune tolerance. However, mice T cells lacking general control nonderepressible 2, an amino acid sensor, are not susceptible to IDO-mediated anergy by dendritic cells in tumor-draining lymph nodes,[13] suggesting that IDO may mediate immune response functions via tryptophan catabolites, and tryptophan itself. However, the immune activation effects of tryptophan accumulation, another possible outcome of IDO inhibition, have largely been ignored.

T lymphocytes are extremely sensitive to tryptophan shortage, which causes their

arrest in the G1 phase of the cell cycle.[14] By depleting tryptophan in local tissue environments, IDO sensitizes T cells to apoptosis.[14] IDO knockout (KO) in mice greatly sensitized them to PD-L1 antibody treatment to B16 melanoma tumor growth and increased overall survival.[15] In patients with advanced non-small cell lung cancer, higher IDO activity could predict resistance to anti-PD-1 treatment.[16] In advanced glioblastoma, IDO inhibition was reported to synergize PD-1-blockade to improve survival.[17] All these facts suggest an intrinsic connection between IDO and PD-1, and a possibility of the inhibitory function of IDO via mediation of PD-1 expression. However, whether tryptophan shortage would induce PD-1 upregulation, an event that promotes T cell apoptosis,[18] is yet to be revealed.

Besides being building blocks of biosynthesis, tryptophan and other amino acids are signaling molecules that regulate various biological processes through transfer RNA (tRNA) synthetase catalyzed lysine modifications in proteins.[19 20] Thus, it is important to investigate whether tryptophan, in addition to its catabolites, is a regulator of immunity. In the current study, we report that tryptophan boosts the immunity of T cells, which decreases T cell surface PD-1 expression via tryptophanylation of E3 ligase TRIP12.

MATERIALS AND METHODS
Plasmid constructs
The *TRIP12* complementary DNA (cDNA) (NM_001284214.2) was a generous gift from Jiahuai Han's lab (Xiamen University, China). *TRIP12* cDNA was cloned into pCMV-flag or pCMV-myc vector. *TRIP12* mutants were generated by Fast Mutagenesis Kit (Vazyme, Nanjing, China) following the manufacturer's instructions. The pENTER-NFATc1-flag plasmid was purchased from Vigene Biosciences (Shandong, China) and *NFATc1* (NM_172390.3) was subcloned into pCMV-myc vector. The pCMV-ubiquitin (Ub)-HA, pcDNA3.1-WARS-flag, pcDNA3.1-SIRT1/2/3/4/5/6/7-HA plasmids were constructed previously in our laboratory. Tryptophanyl-tRNA synthetase (*WARS*) (NM_173701.2) cDNA was cloned into pCMV-flag or pCMV-myc vector to obtain WARS expression plasmids. The sgRNAs for *WARS/TRIP12* KO were inserted into pSpCas9(BB)-2A-Puro vector and the sgRNAs for *TRIP12* knockin were inserted into pSpCas9(BB)-2A-GFP. All constructs were confirmed by sequencing.

Antibodies
Commercial antibodies
For human and mouse CD8$^+$ T cell activation, antihuman CD3, antihuman CD28, antimouse CD3 and antimouse CD28 were purchased from Biolegend (San Diego, California, USA). For flow cytometry analysis, antimouse CD16/32, fluorescein isothiocyanate (FITC) antimouse CD45, APC antimouse CD3, Alexa Fluor 488 antimouse CD3, PerCP/Cyanine5.5 antimouse CD4, Brilliant Violet 421 antimouse CD8a, PE antimouse CD8a, PE antimouse PD-1, APC antihuman CD3, FITC antihuman PD-1, PE antihuman interferon (IFN)-γ, APC antihuman tumor necrosis factor (TNF)-α, PerCP/Cyanine5.5 antimouse granzyme B, PE antimouse perforin, zombie aqua, Alexa Fluor 700 antimouse anti-CD8, Alexa Fluor 647 antimouse TCR-Va2, FITC antimouse KLRG1 and PE antimouse CD127 were purchased from Biolegend. eFluor450 antimouse TNF-α was purchased from eBiosciences (San Jose, USA). PE-Cy7 antimouse IFN-γ was purchased from BD Biosciences (San Diego, USA). For western blot analyses, anti-TRIP12 was purchased from Bethyl Laboratories (Montgomery, Texas, USA), anti-NFATc1 was from Santa Cruz Biotechnology (Shanghai, China), anti-WARS was from Proteintech (Hubei, China), anti-actin was from Sigma (St. Louis, Missouri, USA), anti-IDO1 was from Proteintech and Cell Signaling Technology (New England Biolabs, Ipswich, Massachusetts, USA), anti-HA-horseradish peroxidase (HRP) was from MBL (Nagoya, Japan), anti-flag-HRP, anti-myc-HRP was from GNI (Tokyo, Japan), HRP-conjugated goat antirabbit, HRP-conjugated goat antimouse were from Jackson ImmunoResearch (West Grove, Pennsylvania, USA). For immunofluorescence, antimouse CD4, antimouse CD8 were purchased from Biolegend, Alexa Fluor 647-affinipure goat antirat IgG (H+L) was from Jackson ImmunoResearch. For immunoprecipitation, anti-flag M2 agarose beads were purchased from Sigma, anti-myc was from Abcam (Cambridge, Massachusetts, USA). Anti-PD-1 was purchased from Bio X Cell (clone RMP1-14, West Lebanon, New Hampshire, USA).

Preparation and validation of tryptophanylation antibodies
Antitryptophanylation antibody (TrpK) was customized from Abmart (Shanghai, China). It was raised in rabbits against the synthetic peptide containing tryptophanylated lysine residues (Ac-CGGGK(w)GGGK(w)GGGK(w)GGG-NH$_2$, TrpK-W). Rabbits were injected with the TrpK-W for 3 times and exsanguinated 10 days following the final boost. Tryptophanylation antibodies (anti-Trp-K) from antisera were captured and purified.

To validate the anti-Trp-K, dot blot assays were conducted to test the reactivity of anti-Trp-K against TrpK-W and a synthetic peptide with identical amino acid sequence but devoid of tryptophanylation (Ac-CGGGKG-GGKGGGKGGG-NH$_2$). The specificity of anti-Trp-K was tested by competing anti-Trp-K binding to TrpK-W with tryptophanylated bovine serum albumin, which was made according to a protocol described by Moellering and Cravatt.[21] Briefly, the lysine tryptophanylation reactions were carried out at room temperature in a 2 mL reaction mix (2-(N-Morpholino)ethanesulfonic acid potassium salt (MES) base, pH 7.5) that contains 3.4 mg/mL tryptophanylation, 35 mg/mL 1-(3-Dimethylaminopropyl)-3-et hylcarbodiimide hydro (EDC) (Thermo Fisher Scientific, Waltham, Massachusetts, USA), and 40 mg/mL N-Hydroxy succinimide (NHS) (Thermo Fisher Scientific).

BSA solution was added to a final concentration of 1 mg/mL.

Cells
HEK293T, Jurkat T, CT26, Lewis lung carcinoma (LLC), and B16F10 cell lines were originally purchased from the Cell Bank of the Chinese Academy of Sciences.

Generation of WARS knockout, TRIP12 knockout, and knockin HEK293T cells
HEK293T-*WARS*-KO, HEK 293T-*TRIP12*-KO and HEK 293T-*TRIP12-K1136R*-knockin cell lines were generated using CRISPR-Cas9 KO/knockin strategy. The sgRNAs were designed from the website (http://crispr.mit.edu) and then the sgRNAs for HEK293T-*TRIP12/WARS*-KO cells were inserted into pSpCas9(BB)-2A-Puro and the sgRNAs for HEK293T-*TRIP12-K1136R*-knockin cells were inserted into pSpCas9(BB)-2A-GFP vector.

Donor DNA for HEK293T-*TRIP12-K1136R*-knockin was constructed by the following method: The 2199 bp fragments spanning from 1140 bp upstream and 1056 bp downstream with site K1136R (AAA) of *TRIP12* gene were amplified from genomic DNA which was extracted from HEK293 cells, and cloned into pCMV-flag vector. K1136 AAA was mutated into K1136R CGC using Mut Express II Fast Mutagenesis Kit V2 (Vazyme).

HEK293T cells were transfected with the constructed plasmid using Lipofectamine 3000 (Thermo Fisher Scientific). Two days later, HEK293T-*TRIP12/WARS*-KO cells were selected with 2 μg/mL puromycin (sigma) for a week and GFP-positive HEK293T-*TRIP12-K1136R*-knockin cells was isolated by fluorescence-activated cell sorting. Single cell clones were then obtained in 96-well plates. KO and knockin cells were verified by sequencing and western blot analysis.

Preparation of mouse CD8$^+$ T cells
Mice were sacrificed by rapid cervical dislocation and the body surface was sterilized in 75% alcohol. Maintaining in a sterile environment, spleen without extra fat was dissociated and collected using sterile forceps and scissors. The spleens were washed by phosphate buffered saline (PBS) and crushed to isolate spleen cells by grinding the spleens with a syringe plunger against 70 μm nylon mesh filter, and red blood cells were lysed using red cell lysis buffer. Splenocytes without red blood cells were filtered with 70 μm nylon mesh filter, centrifuged at 2000 rpm for 5 min and washed 3 times by staining buffer (PBS+0.5% fetal bovine serum (FBS)). Then, the CD8$^+$ T cells of splenocytes were acquired by mouse CD8-naïve T cell isolation kit (Biolegend). Briefly, after washed by matching MojoSort buffer 3 times, splenocytes were resuspended in MojoSort buffer at a concentration of 1×10^8 cells/mL. Each 100 μL cell suspension was mixed with 10 μL matching biotin-antibody cocktail and incubated for 15 min. Then, 10 μL matching streptavidin nanobeads were added into the above mixture and incubated for 15 min. Then, 2.5 mL MojoSort buffer was added, the mixture was transferred to the flow cytometry tube and the tube was placed in the magnet for 5 min. Finally, the liquid which contains mouse-naïve CD8$^+$ T cells were collected.

For specific cytotoxicity assays, CD8$^+$ T cellsfrom OVA-immuned BALB/c mice were acquired by flow cytometry cell sorting. Briefly, unconjugated antimouse CD16/32 was used for blocking Fc receptors. After stained by antimouse CD3 and CD8 for 30 min, splenocytes was washed 3 times and resuspended using staining buffer. Finally, CD3$^+$CD8$^+$ dual positive cells were selected by flow cytometric cell sorting.

Cells culture and plasmid transfection
HEK293T, LLC, and CT26 cells were cultured in complete Dulbecco's Modified Eagle Medium medium (Hyclone, Logan, Utah, USA) supplemented with 10% FBS (Bioind, Israel) and antibiotics (100 μg/mL streptomycin and 100 units/mL penicillin, Gibco, Paisley, UK), Jurkat T cells were cultured in RPMI 1640 medium (Hyclone) containing 10% FBS and streptomycin/penicillin. Mouse CD8$^+$ T cells were cultured in complete RPMI 1640 medium containing 10% FBS, antibiotics and interleukin (IL)-2 (10 ng/mL). All cells were maintained at 37°C in humidified 5% CO$_2$.

Plasmids were transfected into adherent cells using polyethylenemine (PEI) (1 μg/μL, Polysciences, Warrington, USA), small interfering RNAs (siRNAs) were transfected into adherent cells by HilyMax (Dojindo Molecular Technologies, Kumamoto, Japan). Transfection of Jurkat T was performed through electroporation by Lonza Amaxa Nucleofector 2B (Lonza, Basel, Switzerland) with program S-018.

T cells activation
Cell culture plates were pre-coated with anti-CD3 and anti-CD28 antibodies at 4°C overnight, and then washed 3 times with RPMI 1640 medium. Jurkat T or mouse-naïve CD8$^+$ T cells were activated with the pre-coated plates for 2 days.

Jurkat T cell proliferation
Proliferation was measured by flow cytometry using carboxyfluorescein diacetate succinimidyl ester (CFSE) (eBioscience). Briefly, Jurkat cell suspensions (1×10^7 cells) were prepared and labeled with 0.5 μM CFSE at 37°C for 10 min, washed with RPMI 1640 medium containing 50% FBS, and then resuspended in pre-warmed cell culture medium containing 10% FBS. Forty-eight hours later, dividing cells were detected by flow cytometry and cell proliferation was quantified by CFSE dilution.

Cell treatments
IDO inhibitors
For IDO inhibitors treatment, Jurkat T cell were treated with indoximod (CAS No. 110117-83-4), epacadostat (CAS No. 1204669-58-8) or NLG919 analog (CAS No. 1402836-58-1) (Selleck Chemicals, Houston, Texas, USA) for 6–8 hours in different concentration as indicated in the figures or legends.

Tryptophan starvation

Tryptophan starvation was performed in HET293T, Jurkat T cells, and mouse $CD8^+$ T cells. Cells were cultured in Trp-free RPMI 1640 medium (Yeasen Biotechnology, Beijing, China) at 37°C in humidified 5% CO_2.

Me-Trp and kynurenine supplementation

Cells were first Trp-starved for 2 hours, and then cultured in the medium supplemented with Me-Trp in different concentrations as indicated in the figures or legends for 4–6 hours. Kynurenine supplementation was performed the same way as that of tryptophan supplementation.

Tryptamine and nicotinamide treatments

As for tryptamine and nicotinamide (NAM) treatments, cells were cultured in normal medium supplemented with tryptamine in different concentrations as indicated in the figures or legends or NAM (5 mM) for 6 hours.

NFATc1 half-life analyses and MG132 treatments

To analyze half-life of NFATc1, the culture growth medium was replaced with normal growth medium containing 50 µg/mL cycloheximide, and collected at different time points (0, 1, 2, 4 hours). To inhibit proteasomal degradation of NFATc1, cells were treated with normal growth medium containing 20 µM MG-132 for 6 hours.

Reverse transcription quantitative PCR

Total RNA for reverse transcription quantitative PCR (RT-qPCR) was extracted using Trizol reagent. Following the manufacturer's instruction, RT was performed with PrimeScript RT reagent kit (Takara, Tokyo, Japan) and qPCR was performed using AceQ qPCR SYBR Green Master Mix (Vazyme). Quantitative analysis of qPCR was carried out by $2^{-\triangle\triangle Ct}$ method used *actin* as the internal reference indicator.

Western blot analysis

Cells were lysed with sodium dodecyl sulfate (SDS) protein sample loading buffer or lysed in 0.5% NP-40 lysis buffer (50 mmol/L Tris-HCl, 150 mmol/L NaCl, 0.5% NP-40, pH=7.2–7.4, protease inhibitors cocktail tablets (Roche, Indianapolis, Indiana, USA)) at 4°C for 30 min. Protein was separated using SDS-PAGE in appropriate gel concentration by electrophoresis according to the molecular weight of the target protein, and then transferred onto nitrocellulose (NC) membranes. Membranes were blocked with 5% non-fat milk in triethanolamine buffered saline (TBS) containing 0.05% Tween-20, and incubated overnight at 4°C with primary antibodies (actin, 1:10,000; NFATc1, 1:200; TRIP12, 1:1000; WARS, 1:1000; IDO1, 1:1000). The blots were washed, incubated in peroxidase-coupled secondary antibodies against rabbit or mouse IgG (1:5000) at room temperature, then washed and developed using Super Signal Substrate (CLiNX, Shanghai, China). The Myc-tagged or Flag-tagged or HA-tagged proteins were detected with HRP-labeled primary antibodies (anti-HA-HRP, 1:2000; anti-flag-HRP, 1:2000; anti-myc-HRP, 1:2000). Signal intensity was visualized by ChemiScope 3300 Mini Imager Systems (CLiNX).

Enzyme-linked immunosorbent assay

The ELISA kit for testing TNF-α, IFN-γ was purchased from Biolegend. Cell culture supernatants were collected and the cytokines were assessed according to the manufacturer's instructions. Capture antibody solution was added to microplate wells and incubated overnight (16–18 hours) between 2°C and 8°C. Assay diluent buffer was used to block non-specific binding. Serially diluted protein standard or test sample were incubated for 2 hours at room temperature with shaking. The trapped antibody was then added and detected by substrate solution. Optical density of each well was determined within 20 min using a microplate reader set to 450 nm.

The ELISA kit for ovalbumin (OVA)-sIgG was purchased from Jining Industrial (Shanghai, China). Blood samples were collected from the orbital venous plexus of mouse, and were left to stand for 1 hour at room temperature, then centrifuged at 1500 rpm for 20 min to separate serum. The OVA-sIgG was measured according to the manufacturer's instructions.

Immunoprecipitation

Beads used in the immunoprecipitation were washed and equilibrated in 0.1% NP-40 lysis buffer. Briefly, cell lysates were prepared using immunoprecipitation assay buffer (50 mmol/L Tris-HCl, 150 mmol/L NaCl, 0.1% NP-40, pH=7.2–7.4, protease inhibitors cocktail tablets (Roche)) for 30 min at 4°C, then incubated with anti-flag beads (Sigma) to enrich the target protein overnight at 4°C. For immunoprecipitaion of TRIP12-myc protein, the cell lysates were first incubated with anti-myc antibody overnight at 4°C, followed by 4 hours incubation with protein A/G plus-agarose beads. The beads were then washed vigorously with immunoprecipitation lysis buffer for 6–8 times. The protein was eluted by boiling the beads with SDS loading buffer for 5 min, and then subjected to western blot analysis.

In vivo ubiquitination assay

Plasmids ubiquitin-HA, NFATc1-flag, and TRIP12-WT-myc, or TRIP12-K1136R/W-myc, or TRIP12-ΔHECT-myc were co-transfected into HEK293T cells. The HEK293T cells were treated with 20 µM MG-132 for 6 hours before harvest. NFATc1 was purified by co-immunoprecipitation using anti-flag-conjugated agarose beads (Sigma), followed by western blot analysis. To examine the effect of WARS on ubiquitination of NFATc1, *siWARS* were co-transfected with ubiquitin-HA, NFATc1-flag, and TRIP12-WT-myc in HEK293T cells. Alternatively, WARS were reintroduced into HEK293T-*WARS*-KO cells by co-transfection with ubiquitin-HA, NFATc1-flag, and TRIP12-WT-myc.

Mice tumor models

Female C57BL/6 mice aged 4 weeks were purchased from SLAC Laboratory Animal (Shanghai, China). The

mice were housed in a standard environment and fed with a standard diet during a 1-week adaptation period. The LLC cells or B16F10 cells of logarithmic phase were harvested, and single cell suspensions were prepared. Healthy female C57BL/6 mice, weighing 18–20 g, were subcutaneously inoculated in the left axillae with 5×10^5 LLC cells or B16F10 cells. The day after inoculation, the mice were randomly divided into four groups, 10 mice in each group. For LLC-inoculated mice, the Me-Trp group received an intraperitoneal injection of Me-tryptophan solution (≈150 mg/kg, dissolved in PBS), and indoximod group received an intraperitoneal injection of indoximod suspension liquid (≈100 mg/kg, dissolved in NaOH solution, pH adjusted to 7.2–7.4). The Me-Trp and indoximod group were intraperitoneally injected with both Me-Trp (≈150 mg/kg, dissolved in PBS) and indoximod (≈100 mg/kg). The corresponding control mice received an equivalent volume of PBS. All the injections were performed twice per day (09:00 and 17:00 hours). For B16F10-inoculated mice, Me-Trp and control group were the same as that in LLC-inoculated mice. Anti-PD-1 (10 mg/kg) were administered by intraperitoneal injections on days 3, 6, 9, and 12 after inoculation in anti-PD-1 group. The anti-PD-1 and Me-Trp group was injected with both anti-PD-1 and Me-Trp. Tumor sizes were measured 2 or 3 times a week by randomizing the order, with each mouse tested within an hour on the same day. The tumor volume was calculated by the following formula: tumor volume=0.5×tumor length×tumor width×tumor width. Mice were excluded if they died or if their tumors ruptured, or the tumor volume exceeded 1 cm^3. The tumor-bearing mice were sacrificed by cervical dislocation. Tumors and spleen were carefully removed, and tumors were weighed and photographed.

Flow cytometry
Surface staining of PD-1
For the preparation of mice-naïve CD8$^+$ T cells, or CD8$^+$ cells from OVA-immuned mice, or tumor-infiltrating CD8$^+$ T cells from CLL-bearing mice, splenocytes were obtained with the same method as described above. Mouse tumors were minced with scissors and subjected to enzymatic digestion with 2 mg/mL collagenase type I (Stem Cell Technologies, Vancouver, Canada) in 37℃ with shaking for 2 hours, and cells were filtered through a 70 µm nylon mesh filter. To analyze the PD-1 surface expression of mouse CD8$^+$ T cells, cell aggregates, small debris and dead cells were excluded on the basis of forward-scatter and side-scatter, then leukocytes were distinguished by a CD45$^+$ cell gate, then T cells were distinguished by a CD3$^+$ cell gate, then a CD8$^+$ cell gate was used to define CD8$^+$ T cells using Beckman Coulter Gallios flow cytometer (Fullerton, California, USA). Compensation was made according to single staining. The mouse CD8$^+$ cells were blocked by anti-CD16/32 at 4℃ for 10 min, then stained with antibody against PD-1 at 4℃ for 30 min before subjecting to flow cytometer. As for Jurkat T cells, PBS containing 5% FBS was used for blocking. After cell aggregates, small debris and dead cells were excluded on the basis of forward-scatter and side-scatter, a single stain of PD-1 surface expression of Jurkat T was analyzed by FlowJo software (Tree Star, San Carlos, California, USA). Cells stained with isotype control antibody were considered as negative control. Percentage of PD-1-positive cells was determined in comparison to isotype control antibodies. The PD-1 mean fluorescence intensity (MFI) was calculated.

Intracellular staining of IL-2, TNF-α, and IFN-γ, granzyme B, and perforin
Activated Jurkat T cells were treated by brefeldin A for 6 hours before collecting, fixed in 4% paraformaldehyde for 20 min at room temperature, permeabilized with intracellular staining wash buffer (Biolegend), cells were blocked with PBS containing 5% PBS, IL-2, TNF-α, IFN-γ were then stained.

Splenocytes were subjected to erythrocyte lysis buffer and prepared by passing spleen tissue through a 70-µm cell strainer, and then treated by cell stimulation cocktail (eBioscience) and brefeldin A (Biolegend) for 6 hours. After stained with zombie aqua and the surface markers, splenocytes were fixed in fixation buffer (Biolegend) for 20 min at room temperature, permeabilized with intracellular staining wash buffer, blocked with anti-CD16/32, and then stained with anti-IFN-γ, granzyme B, and perforin.

Appropriate isotype controls were used, and compensation was made according to single staining. Percentage of positive cells and MFI were analyzed with FlowJo software (Tree Star).

Immunofluorescence
Tumors removed from sacrificed mice were fixed for 3 days with 4% paraformaldehyde at 4℃, and then placed in 30% sucrose solution for 2 days for dehydration. The samples and cryostat microtome were prechilled to −20℃, and then tumor sections (45 µm) were cut on a cryostat microtome, blocked with 5% goat serums in PBS containing 0.1% Triton X-100 for 2 hours, and then incubated with primary antibodies (CD4, 1:150; CD8, 1:150) in blocking buffer overnight. Subsequent to the excess primary antibody being washed off, sections were incubated with Alexa Fluor 647-labeled goat antirat IgG (Jackson ImmunoResearch, 1:200) and DAPI for 3 hours. The sections were sealed with antifluorescence quencher. After standing for a few days, fluorescence was visualized and images along the z-axis (z-axis interval: 2 µm) were captured by Olympus FV3000 inverted confocal microscope (Centre Valley, Pennsylvania, USA) equipped with a 40× objective lens. The cell number of positive signals per cubic millimeter was calculated.

Cytotoxicity assays
For specific cytotoxicity assays, CD8$^+$ T cells isolated from OVA-immuned BALB/c mice were used as effector cells. Emulsified OVA protein was injected into BALB/c mice by three subcutaneous injections at 1-week or 2-week intervals.

CD8$^+$ T cells were obtained from spleens by flow cytometric sorting with surface markers CD3 and CD8. Then CD8$^+$ T cells were treated with tryptophan in different concentrations. Target mouse cancer cell lines LLC and CT26, which were placed in the U-type 96-well plate in advance, were soaked with 10 µM OVA peptide (SIINFEKL) at 37°C for 1 hour. Excess OVA peptide was washed away by RPMI 1640 medium, then CD8$^+$ T cells were added and co-cultured with target cancer cells at E:T ratios of 10:1. Subsequently, floating CD8$^+$ T cells from the supernatant were washed off by PBS, the remaining adherent cancer cells were digested by 0.25% trypsin, washed by PBS for 3 times, and stained using an annexin V-FITC/propidium iodide apoptosis kit (TaKaRa, Dalian, China). Apoptosis of target cancer cells was measured with Beckman Coulter Gallios flow cytometer to reflect the cytotoxicity ability of CD8$^+$ T cells. A CD3 staining was used to distinguish CD3$^-$ cancer cells and the remaining CD3$^+$ CD8$^+$ T cells.

T cells adoptive transfer

For adoptive T-cell transfer, CD8$^+$ T cells were isolated from spleens and lymph nodes of ovalbumin-transgenic (OT-1) mice (kindly provided by Dr Xiaofei Yu of Fudan University) with mouse CD8$^+$ T cells isolation kit (Biolegend, San Diego, California, USA), and then transferred into recipient C57BL/6 WT mice (2×10^6 cells/mouse) by intravenous injection. The next day, each mouse was immunized by subcutaneous multiple-point injections with 20 µg OVA (Sigma-Aldrich) diluted in 100 µL PBS that mixed with 100 µL complete Freund's adjuvant (Sigma-Aldrich). Me-Trp (150 mg/kg) or indoximod (100 mg/kg) was administered by intraperitoneal injections twice a day. NFAT inhibitor VIVIT peptide (10 mg/kg) (MCE, Monmouth Junction, New Jersey, USA) was intraperitoneally injected once a day. All the treatments were started 1 day before adoptive transfer (day 0) until sacrifice.

In vivo T cell differentiation

Day 8 after adoptive transfer, splenocytes were obtained and stain with zombie aqua (Biolegend), anti-CD8 (Biolegend), anti-TCR-Va2 (Biolegend), anti-KLRG1 (Biolegend), and anti-CD127 (Biolegend). Short-lived effector CD8$^+$ T cells and memory precursor effector cells were distinguished by KLRG1 and CD127 staining.

SIRT1 knockout mice

Whole-body SIRT1 knockout (SIRT1-KO) mice and the corresponding control mice were were generated by the Cre/loxP recombination system. *SIRT1*-KO mice (Cre$^+$ *SIRT1*$^{flox/flox}$) were generated by crossing homologous *SIRT1*$^{flox/flox}$ (Southern Model Organisms, Shanghai, China) with *UBC-Cre-ERT2* mice (Southern Model Organisms). The control mice (wild type (WT)) were *SIRT-1*$^{flox/flox}$ (Cre negative). Activation of Cre recombinase was induced by intraperitoneal injection of tamoxifen (Sigma). Tamoxifen was dissolved in corn oil containing 10% ethanol (20 mg/mL) at 37°C, stored at −20°C and protected from light. Each mouse was administered 100 µL of tamoxifen solution per day for seven consecutive days by intraperitoneal injection. Mice were tested after a recovery period of at least 1 week after the final tamoxifen injection to permit deletion of the *SIRT1* gene and degradation of residual SIRT1 and *SIRT1* messenger RNA (mRNA). PCR and western blot analysis were used to confirm the efficiency of Cre-loxP-mediated SIRT1 deletion in splenic tissue. The DNA was extracted from splenic tissue using Genomic DNA Extraction Kit (TIANGEN, Shanghai, China) according to the manufacturer's protocol, and then PCR was performed to identify mice with Cre recombinase and *SIRT1* loxP sites.

Oligonucleotides

siRNA *TRIP12*-A: GACAAAGACUCAUACAAUAUU
siRNA *TRIP12*-B: GAACACAGAUGGUGCGAUAUU
siRNA *NFATc1*-A: CCCGUUCACGUCAGUUUCUACGUCU
siRNA *NFATc1*-B: CGAGCCGUCAUUGACUGUGCCGGAA
siRNA *WARS*-A: CCAGGAUCCUUACUUUAGAdTdT
siRNA *WARS*-B: GGUUCUUGAUGCCUAUGAAdTdT
CRISPR/Cas9-mediated *TRIP12* gene KO sgRNA-A: CACCGCAACCACAAGACGACTCAAT
CRISPR/Cas9-mediated *TRIP12* gene KO sgRNA-B: CACCGCTGGAACAACACTCTTGAC
CRISPR/Cas9-mediated *WARS* gene KO sgRNA: CACCGAACTGCCCAGCGTGACCAG
CRISPR/Cas9-mediated *TRIP12-K1136R* gene knockin sgRNA-A: CACCGTAAAGGTTGGATTAAGGAGC
CRISPR/Cas9-mediated *TRIP12-K1136R* gene knockin sgRNA-B: CACCGTCTTGTAGAGAAAAAATTAA
Q-PCR *NFATc1*-F: AAAACTGACCGGGACCTGTG
Q-PCR *NFATc1*-R: GCTCATGTTCACGGCTTACG
Q-PCR *PD-1*-F: CCAGGATGGTTCTTAGACTCCC
Q-PCR *PD-1*-R: TTTAGCACGAAGCTCTCCGAT
Q-PCR *actin*-F: CCTCTCCCAAGTCCACACAG
Q-PCR *actin*-R: GGGCACGAAGGCTCATCATT

Statistical analysis

Statistical analyses and graphs were undertaken using GraphPad Prism V.8.0 (GraphPad Software, San Diego, USA). The mean values±SD of independent experiments triplicates and every data point were shown in graph. Unpaired two-sided Student's t-test was used to reflect the difference between two groups.

Results infigures 1B, online supplemental figure S1A–H, S2B-D, S2F, S2G, S3A, S3C–G, S3J, S4G–H, S6A–C, S6E, 7A–B, 7I are representative data of three independent repeats. And there were similar results in three independent repeats.

RESULTS
Tryptophanyl-tRNA synthetase-dependent downregulation of PD-1 expression by tryptophan

In immortalized anti-CD3 and anti-CD28 antibodies co-stimulated Jurkat cells (online supplemental figure S1A), L-methyl-tryptophan ester (Me-Trp) administration
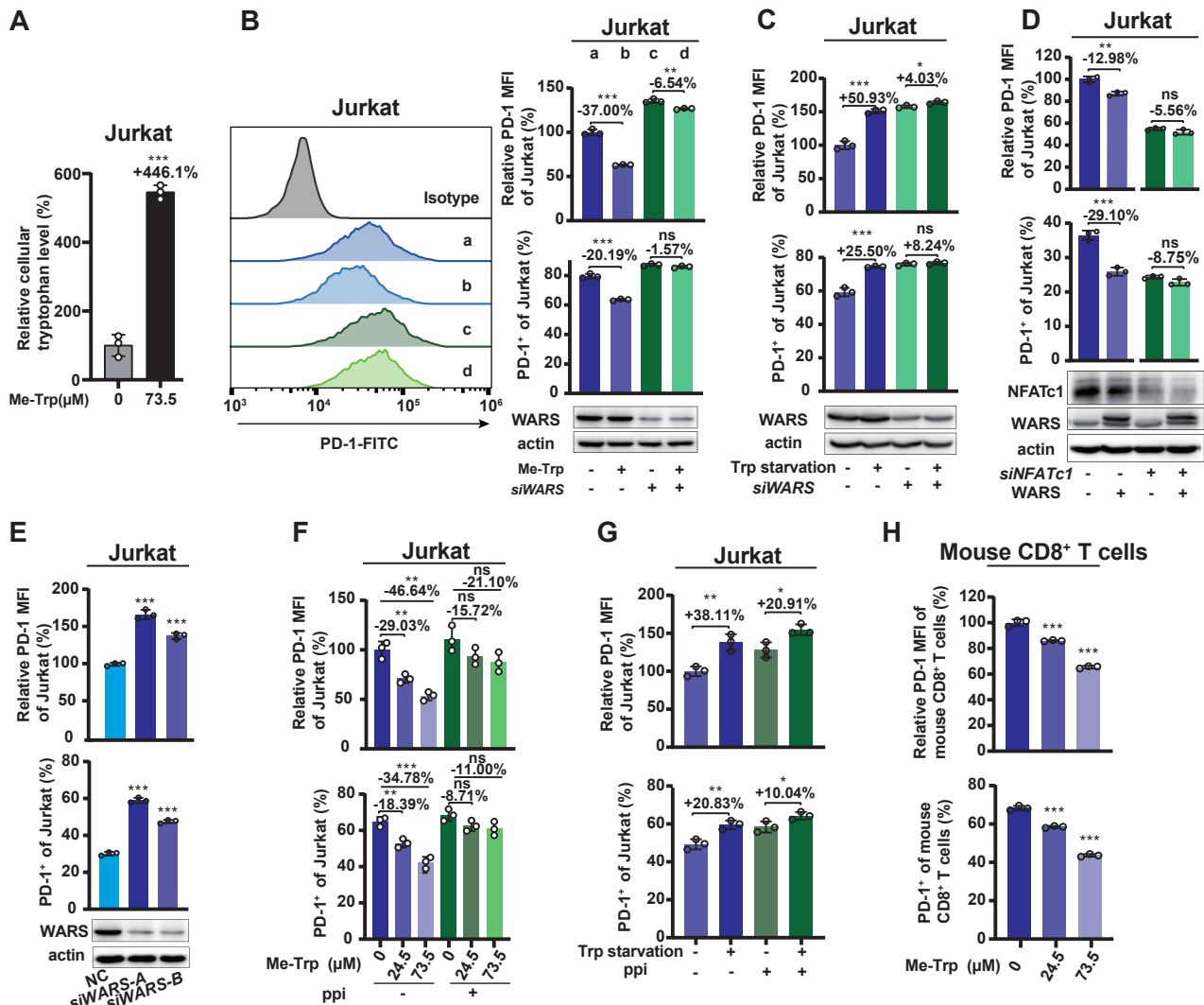
Figure 1 Tryptophan tryptophanyl-tRNA synthetase (WARS)-dependently downregulated programmed cell death protein 1 (PD-1) expression. (A) Me-Trp administration increases intracellular tryptophan. Anti-CD3 and anti-CD28 antibodies co-stimulated Jurkat T cells were supplemented with 73.5 µM L-methyl-Trp in the culture media. The levels of intracellular tryptophan were detected by liquid chromatography-mass spectrometry. n=3, mean±SD. Knockdown *WARS* abrogated cell surface PD-1 regulation by Me-Trp. The cell surface PD-1 levels were detected by mean fluorescence intensity (MFI, herein after) and percentage of PD-1+ cells in Jurkat cells and Jurkat cells with WARS knocked down by small interfering RNAs (siRNAs) when Me-Trp supplemental (B) or tryptophan-deprivation (C) were applied to cells. All levels were compared with that of Jurkat cells without treatment. n=3, mean±SD. Silencing *NFATc1* diminished WARS ability to alter cell surface PD-1. The PD-1 expression levels were detected in Jurkat T cells and *NFATc1* knockdown Jurkat T cells under either WARS overexpression (D) or *WARS* knockdown (E). MFI levels and PD-1-positive cell levels were calculated and compared with that of the controls. n=3, mean±SD. Pyrophosphate (ppi) inhibited Me-Trp supplemental and tryptophan-starvation to alter PD-1. The PD-1 expression levels were detected in stimulated Jurkat T cells that were cultured in media supplemented with Me-Trp (F) or with tryptophan deprived (G) under presence or absence of ppi (10 mM final concentration) in the culture media. n=3, mean±SD. (H) Me-Trp administration decreased mouse CD8+ T cells surface PD-1. Mouse-naïve CD8+ T cells were isolated and activated by anti-CD3/CD28 antibodies (5 µg/mL). The CD8+ T cells surface PD-1 expression levels were detected when they were cultured in media with indicated Me-Trp levels. n=3, mean±SD. *P<0.05, **p<0.01, ***p<0.001, two-tailed Student's t-test.

in culture media at 73.5 µM increased intracellular tryptophan by 446.1% (figure 1A), and decreased the cell surface PD-1 by 37.00% (figure 1B). In contrast, depriving the culture media of tryptophan upregulated PD-1 by 50.93% (figure 1C, online supplemental figure S1B). These results suggest that tryptophan or its catabolites negatively regulate PD-1 expression in Jurkat cells. Since tryptophan can modify lysine residues in proteins and

regulate protein functions,[19] we investigated whether tryptophan inhibited PD-1 expression through lysine tryptophanylation. Overexpression of WARS, the proven lysine tryptophanyl transferase,[19] phenocopied tryptophan to decrease cell surface PD-1 in Jurkat T cells (figure 1D, online supplemental figure S1C). Conversely, silencing *WARS* with *siRNAs* increased surface PD-1 level (figure 1E, online supplemental figure S1D). Administration of

cells with general aminoacylation inhibitor pyrophosphate[19 20] resulted in PD-1 increasing on Me-Trp supplemental (figure 1F, online supplemental figure S1E) and Trp deprivation (figure 1G, online supplemental figure S1F). These findings suggest that WARS-mediated lysine tryptophanylation likely repressed PD-1 expression.

Me-Trp decreased anti-CD3 and anti-CD28 antibodies activated the cell surface PD-1 in mouse CD8^{+} T cells (figure 1H, online supplemental figure S1G and S1H. Notably, when *WARS* was silenced by *siRNAs*, the PD-1 altering potencies of Me-Trp administration (figure 1B) and tryptophan deprivation (figure 1C and online supplemental figure 1B) on surface PD-1 expression were reduced, further supporting that the effects of Trp on PD-1 are mediated by WARS.

IDO inhibitors decreased PD-1 expression by accumulating intracellular tryptophan

The fact that T lymphocytes are extremely sensitive to tryptophan shortage and IDO sensitizes T cells to apoptosis[14] promoted us to examine T cells such as T lymphocyte Jurkat cells express IDO1, as previous studies obtained negative results.[22 23] After activated with anti-CD3 and anti-CD28 antibodies, the levels of IDO1 mRNA increased by >80 folds and the expression of IDO1 was detectable by western blot analysis (online supplemental figure S2A), consistent with a report that Jurkat cells actually expressed IDO1[24] and explained, at least partially, that T cells sensitive to tryptophan levels. As PD-1 expression is restricted to immune cells.[25] We examined a hypothesis that IDO inhibitors may decrease PD-1 expression by elevating intracellular tryptophan levels. Using the IDO inhibitors, namely indoximod, epacadostat, and NLG919 analog at appropriate concentrations increased tryptophan levels and left kynurenine levels negligibly affected in Jurkat T cells (figure 2A), phenocopied Me-Trp supplementation (figure 1B) to decrease the cell surface PD-1 expression in the anti-CD3-activated and anti-CD28-activated Jurkat T cells (figure 2B, online supplemental figure S2B). These, together with that kynurenine had a negligible effect on surface PD-1 expression in Jurkat T cells (figure 2C and online supplemental figure S2C), suggested that tryptophan rather than its catabolites, negatively regulates surface PD-1 expression of Jurkat T cells. Moreover, indoximod has previously been shown to affect T cell function through affecting mammalian target of rapamycin complex 1 (mTORC1) signaling.[26] We tested whether indoximod effects on PD-1 can be independent of mTORC1. Indoximod still able to regulate PD-1 expression (online supplemental figure S2D) when mTORC1 signaling was inhibited by rapamycin in Jurkat cells (online supplemental figure S2E), suggested indoximod may regulate PD-1 in mTORC1-independent mechanisms.

The cell surface PD-1 expression decreasing effects of IDO inhibitors were recaptured in naïve CD8^{+} T cells, isolated from the spleens of BALB/c mice, that were co-treated with anti-CD3 and anti-CD28 antibodies for 48 hours (figure 2D and online supplemental figure S2F). These results suggest that tryptophan decreases surface PD-1 levels through a mechanism other than tryptophan catabolism.

IDO inhibitors increased the levels of IL-2, IFN-γ, and TNF-α, indicators of T cell activation,[27 28] in activated Jurkat cells (figure 2E and online supplemental figure S2G) and in mouse CD8^{+} T cells (figure 2F). These results were consistent with the decrease in PD-1 expression by immunosuppressive tryptophan catabolites.

Tryptophan and WARS downregulated *PD-1* transcription factor NFATc1

RT-qPCR revealed that the mRNA level of *PD-1* was decreased by both Me-Trp and IDO inhibitors treatments in Jurkat cells (figure 3A), suggesting that Me-Trp and IDO inhibitors decrease PD-1 expression level, at least in part, by altering *PD-1* transcription. We tried to identify transcription factors of PD-1 that may be regulated by Me-Trp and IDO inhibitors. Protein levels (figure 3B), but not mRNA levels (figure 3C), of NFATc1, a reported transcriptional factor for PD-1[29] that was confirmed by us (online supplemental figure S3A), were downregulated by Me-Trp supplementation in the culture media for activated Jurkat T cells. Furthermore, tryptophan deprivation of culture media of activated Jurkat T cells increased the protein levels (figure 3D), but not mRNA levels (figure 3E), of NFATc1 of Jurkat cells. These, together with that IDO inhibitors decreased NFATc1 (online supplemental figure S3B) and the cell surface PD-1 expression (see figure 2B), indicate that NFATc1 is regulated by tryptophan and IDO inhibitors, for decreasing cell surface PD-1.

Notably, WARS overexpression, a manipulation that may increase protein tryptophanylation,[19] decreased NFATc1 protein levels (figure 3F), but not *NFATc1* mRNA levels (figure 3G), of Jurkat cells. Moreover, WARS knockdown by *siRNAs* increased NFATc1 protein levels (figure 3H), but not *NFATc1* mRNA levels (figure 3I), of Jurkat cells. These results suggest that tryptophanylation regulates NFATc1 at post-transcription levels. Furthermore, *NFATc1* knockdown, which decreased surface PD-1 expression of Jurkat cells (online supplemental figure S3A), abrogated Me-Trp supplementation (figure 3J, online supplemental figure S3C) to decrease surface PD-1 in Jurkat T cells, indicating that tryptophanylation regulates surface PD-1 expression through NFATc1. These, together with that *NFATc1* knockdown abrogated WARS overexpression and IDO inhibitors to decrease surface PD-1 in Jurkat T cells (figure 1D and online supplemental figure 1C figure 2B and online supplemental figure 2B), confirmed that decreased NFATc1 is the major reason for these manipulations to downregulate surface PD-1 expression.

Compared with that inhibiting NFAT with VIVIT peptide,[30 31] which had no effect on T cell proliferation (online supplemental figure S3D), inhibited IL-2, TNF-α, and IFN-γ production (online supplemental figure S3F), tryptophan supplemental increased IL-2, TNF-α, and IFN-γ production and proliferation (online supplemental figure S3E, S3G) in Jurkat cells. The differences between NFAT inactivation and tryptophan treatment was likely due to that besides decreasing NFATc1 and PD-1 expression to activate T cells, tryptophan supplemental may alter IDO-mediated immunosuppression, which was consistent with the finding
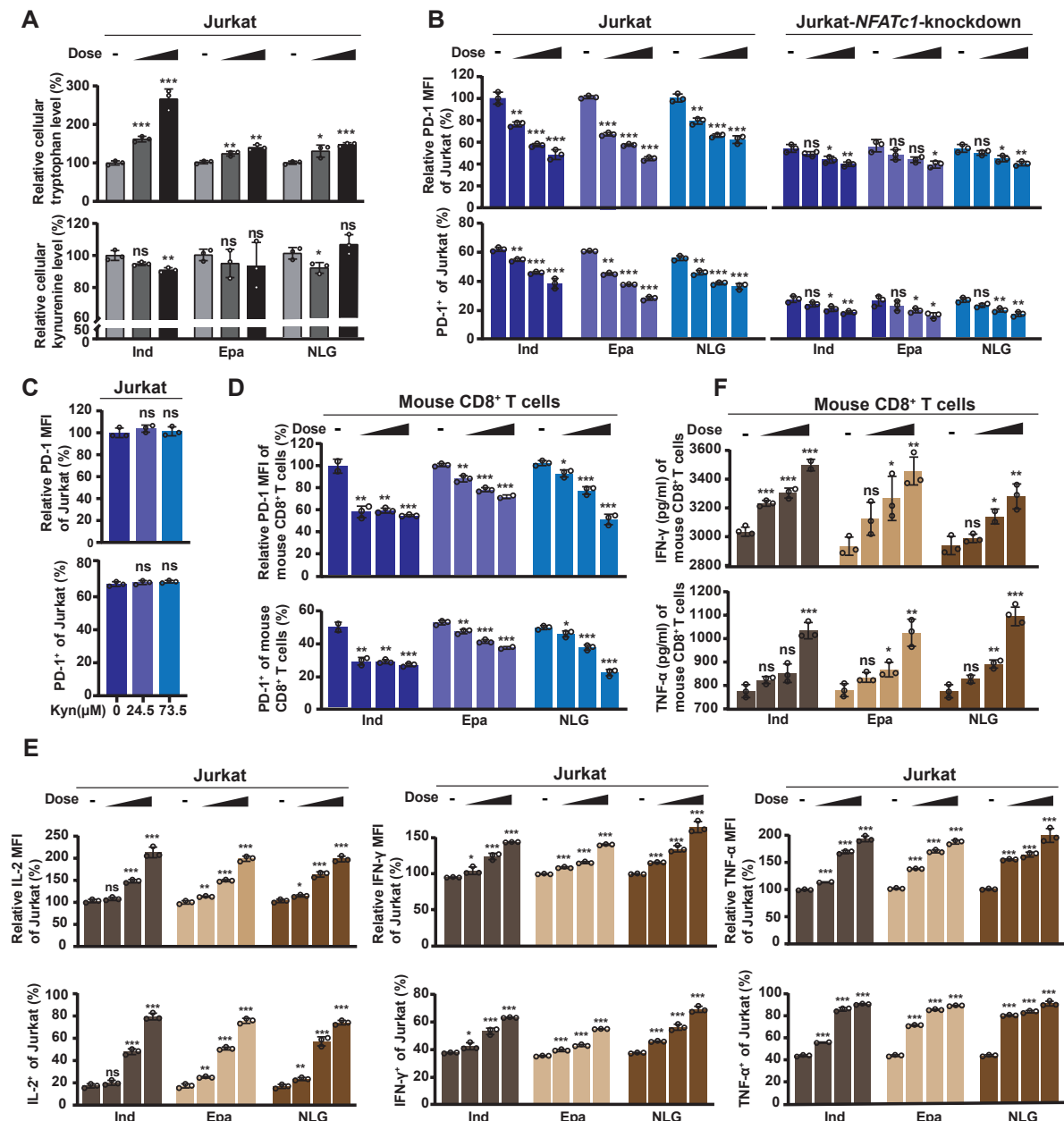
Figure 2 Indoleamine 2,3-dioxygenase (IDO) inhibitors decreases programmed cell death protein 1 (PD-1) through accumulating intracellular tryptophan. (A) IDO inhibitors altered intracellular levels of both tryptophan and kynurenine. Intracellular levels of tryptophan and kynurenine of Jurkat T cells and IDO inhibitors-treated Jurkat T cells were detected by liquid chromatography-mass spectrometry. The final concentrations of IDO inhibitors for indoximod (Ind) were: 0, 10, 50 µM; for epacadostat (Epa) were: 0, 1, 3 µM; and for NLG919 analog (NLG) were: 0, 0.1, 1 µM, respectively. (B) *NFATc1* knockdown prevented IDO inhibitors to decrease PD-1. Cell surface PD-1 mean fluorescence intensity (MFI) and PD-1-positive levels were measured for Jurkat T cells and *NFATc1* knockdown Jurkat T cells that were cultured with presence of indicated levels IDO inhibitors in the culture media. The final concentrations of IDO inhibitors for indoximod (Ind) were: 0, 1, 10, 50 µM; for epacadostat (Epa) were: 0, 0.3, 1, 3 µM; and for NLG919 analog (NLG) were: 0, 0.025, 0.1, 1 µM, respectively (herein after for all dose-dependent experiments of IDO inhibitors in Jurkat T cells). (C) Kynurenine did not affect surface PD-1 expression. Relative cell surface PD-1 MFI levels were measured for Jurkat T cells that were cultured in media supplemented with indicated levels of kynurenine. (D) IDO inhibitors decreased PD-1 in mouse CD8+ T cells. Relative cell surface PD-1 MFI levels and PD-1-positive levels were measured for mouse CD8+ T cells that were cultured with presence of different levels IDO inhibitors in the culture media. The final concentrations of IDO inhibitors for indoximod (Ind) were: 0, 1, 10, 50 µM; for epacadostat (Epa) were: 0, 0.3, 1, 3 µM; and for NLG919 analog (NLG) were: 0, 0.025, 0.1, 0.2 µM, respectively (herein after for all dose-dependent experiments of IDO inhibitors in mouse CD8+ T cells). IDO inhibitors increased interleukin (IL)-2, interferon (IFN)-γ, and tumor necrosis factor (TNF)-α level in T cells. The IL-2, IFN-γ, and TNF-α levels were detected in stimulated Jurkat T cells, IDO inhibitors-treated Jurkat T cells by flow cytometry (E), in mice CD8+ T cells, and IDO inhibitors-treated mice CD8+ T cells by ELISA (F). *P<0.05, **p<0.01, ***p<0.001; ns, not significant.
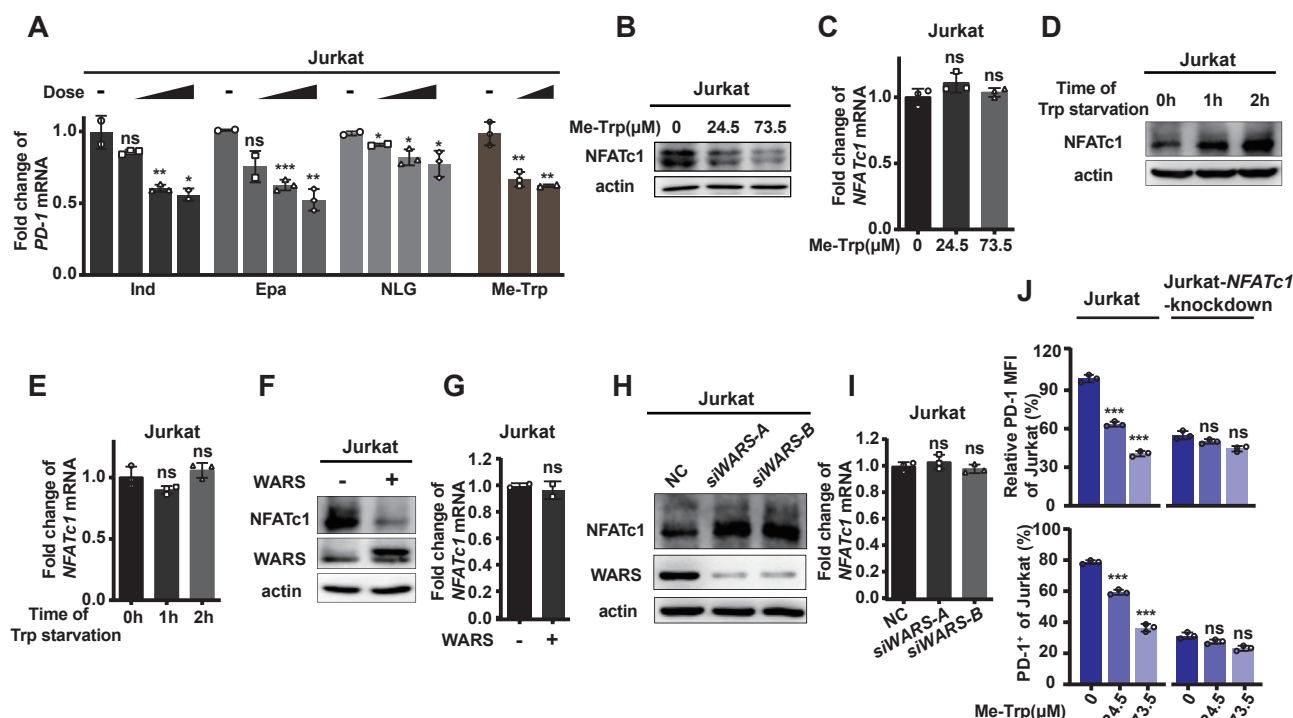
Figure 3 Tryptophan and tryptophanyl-tRNA synthetase (WARS) downregulates programmed cell death protein 1 (PD-1) transcription factor NFATc1. (A) Me-Trp and indoleamine 2,3-dioxygenase (IDO) inhibitors decreased the messenger RNA (mRNA) level of *PD-1* in Jurkat T cells. The *PD-1* mRNA levels of anti-CD3 and anti-CD28 antibodies co-stimulated Jurkat T cells were detected with reverse transcription quantitative PCR (RT-qPCR) when the cells were treated with different levels of indoximod, epacadostat, NLG919 analog, or Me-Trp. Me-Trp supplemental and WARS overexpression decreased the protein level of NFATc1. The protein (B) and mRNA (C) levels of NFATc1 were detected for activated Jurkat T cells that were cultured in media supplemented with indicated levels of Me-Trp. n = 3, mean±SD. Tryptophan starvation increased protein levels of NFATc1. The protein (D) and mRNA (E) levels of NFATc1 were detected at indicated time for activated Jurkat T cells that were cultured in tryptophan-deprived media. n=3, mean±SD. WARS overexpression decreased protein levels of NFATc1. The protein (F) and mRNA (G) levels of NFATc1 were detected in both activated Jurkat T cells and WARS-overexpression activated Jurkat T cells. *WARS* knockdown increased protein levels of NFATc1. The protein (H) and mRNA (I) levels of NFATc1 were detected in both activated Jurkat T cells and WARS-knockdown activated Jurkat T cells. (J) *NFATc1* knockdown abrogated Me-Trp to decrease the cell surface PD-1. The MFI and PD-1-positive Jurkat T cells were detected in Jurkat and NFATc1 knockdown Jurkat cells that were cultured under different levels of Me-Trp. *P<0.05, **p<0.01, ***p<0.001; ns, not significant.

that elevation in circulating tryptophan levels overcome IDO1-mediated immunosuppression in the tumor, along with the IFN-γ mRNA increasing.[32] However, as activated T cell express high levels of IL-2, IFN-γ, and TNF-α,[27 28] which were confirmed in Jurkat (figure 2E and online supplemental figure S2G) and in mouse CD8+ T cells (figure 2F), the increased cytokines in IDO inhibitors may be consequences of T cell activation, a notion that was supported by the fact that both indoximod and tryptophan increased cytokine production (online supplemental figure S3H and S3I) and increased the number of short-lived effector cells (KLRG+CD127−) in C57B6/L mice adoptively transferred with CD8+ isolated from OT-1 mice (online supplemental figure S3H and S3J).

E3 ligase TRIP12 degraded NFATc1 and downregulated PD-1 expression

Proteasome inhibitor MG132 treatment on anti-CD3 and anti-CD28 antibodies co-stimulated Jurkat T cells resulted in elevated NFATc1 protein levels (figure 4A), suggesting that NFATc1 is subject to proteasomal degradation.

Moreover, as MG132 supplementation blocked tryptophan supplementation (online supplemental figure S4A), WARS overexpression (online supplemental figure S4B) and IDO inhibitors (online supplemental figure S4C) decreased NFATc1 levels in Jurkat T cells, suggesting that tryptophanylation regulates NFATc1 levels by altering its proteasomal degradation.

Searching the tryptic peptide library of human liver cancer tissue revealed that lysine 1136 of TRIP12, an E3 ligase, was tryptophanylated (figure 4B), suggesting that TRIP12 may be regulated by tryptophanylation. TRIP12 co-immunoprecipitated with NFATc1, when they were co-expressed in HEK293T cells (figure 4C,D). The half-life of endogenous NFATc1 was prolonged by knockdown of TRIP12 (figure 4E). Deleting *TRIP12* from HEK293T cells (online supplemental figure S4D) decreased the ubiquitination of ectopically expressed NFATc1 (figure 4F). Knockdown of *TRIP12* in Jurkat T cells increased endogenous levels of NFATc1 protein (figure 4E). Furthermore, overexpressing TRIP12, but not a catalytically
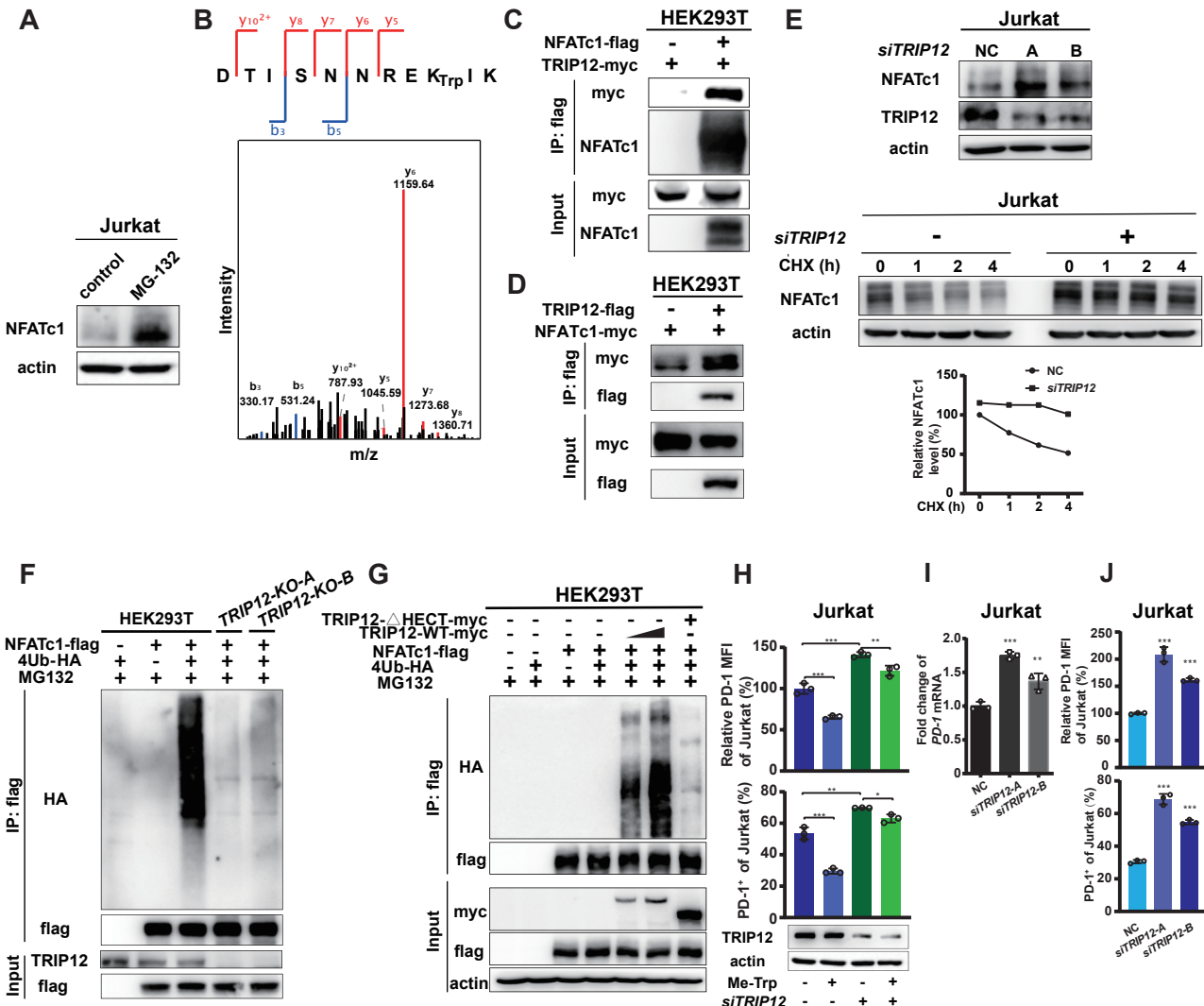
Figure 4 NFATc1 degradation is catalyzed by E3 ligase TRIP12. (A) Proteasome inhibitor MG-132 increased NFATc1 protein levels. The NFATc1 protein levels were detected in Jurkat cells and MG132-tretaed (20 µM) Jurkat cells. (B) Lysine 1136 of TRIP12 was tryptophanylated. A MS/MS spectrum from human liver protein library matched a tryptophanylated TRIP12 peptide (DTISNNREK$_{Trp}$IK). (C, D) TRIP12 interacted with NFATc1. TRIP12 was co-overexpressed with NFATc1 in HEK293T cells. Co-immunoprecipitation experiments were carried out when Flag-tagged NFATc1 or TRIP12 was used as bait. (E) Knockdown *TRIP12* prolonged the half-life of endogenous NFATc1 protein. The protein levels of NFATc1 were measured for Jurkat T cells and *TRIP12* knockdown Jurkat T cells at different time points after cycloheximide (CHX) treatments to block protein synthesis. Cells were transfected with siTRIP12 for 48 hours, followed by 50 µg/mL CHX treatment for 1, 2, and 4 hours. Relative NFATc1 protein levels were quantified against those of the untreated cells. (F) *TRIP12* knockout decreased ubiquitination of ectopically expressed NFATc1. The ubiquitination levels of overexpressed NFATc1 were detected in HEK293T cells and *TRIP12* knockout HEK293T cells. (G) *TRIP12* knockdown increased endogenous NFATc1 protein levels. The protein levels of endogenous NFATc1 were detected in HEK293T cells and *TRIP12* knockdown Jurkat T cells. (H) Impairing TRIP12 catalytic activity abrogated its ability to ubiquitinate NFATc1. NFATc1 was overexpressed alone, or co-overexpressed with TRIP12 or TRIP12 lacking HECT domain (TRIP12-ΔHECT) in HEK293T cells, and ubiquitination levels of NFATc1 were detected. (I) *TRIP12* knockdown abrogated Me-Trp to decrease the cell surface programmed cell death protein 1 (PD-1). The mean fluorescence intensity (MFI) and PD-1positive cells were detected in Jurkat T cells and *TRIP12* knockdown Jurkat T cells when Me-Trp supplemental was applied to cells. n=3, mean±SD. Silencing *TRIP12* elevated cell *PD-1* messenger RNA (mRNA) and surface PD-1 protein. The *PD-1* mRNA levels (J) and the MFI and PD-1-positive cells (K) were detected in Jurkat T cells and *TRIP12* knockdown Jurkat T cells. *P<0.05, **p<0.01, ***p<0.001.

dead TRIP12 with its HECT domain deleted, increased the ubiquitination of NFATc1 (figure 4G) in HEK293T cells, consistent with reduced expression of NFATc1 (online supplemental figure 4E). Furthermore, *TRIP12* KO increased NFATc1 protein levels in HEK293T cells (online supplemental figure S4F). Moreover, knockdown

of *TRIP12* increased PD-1 expression in Jurkat cells (figure 4H and online supplemental figure S4G). These results collectively suggest that TRIP12 is an E3 ligase of NFATc1, which was further substantiated by the knockdown of *TRIP12* in Jurkat T cells elevating cell *PD-1* mRNA (figure 4I) and surface PD-1 protein (figure 4J

and online supplemental figure S4H), whose levels are positively regulated by NFATc1.

Tryptophanylation activated E3 ligase activity of TRIP12

Co-immunoprecipitation revealed that WARS interacted with TRIP12 (online supplemental figure S5A). Moreover, on probing with an antitryptophanylation antibody (online supplemental figures S5B and S5C), WARS overexpression was found to increase tryptophanylation of TRIP12, but not a mutant TRIP12 with K1136 switched to arginine (TRIP12^{K1136R}), which had very low tryptophanylation signal (figure 5A), suggesting that K1136 is the main tryptophanylation site of TRIP12, and allowed us to probe TRIP12 tryptophanylation with the pantryptophanylation antibody. Conversely, taking the advantage that HEK293T cells *WARS* KO (online supplemental figure S5D) was viable as KO other tRNA synthetases such as methionine tRNA synthetase and histidyl-tRNA synthetase 2, we were able to observe that *WARS* KO resulted in decreased NFATc1 ubiquitination (figure 5B) and increased NFATc1 protein levels in HEK293T cells (figure 5C). Tryptamine, a WARS inhibitor,[33] which lowered TRIP12 tryptophanylation levels (online supplemental figure S5E), also decreased NFATc1 ubiquitination in HEK293T cells (online supplemental figure S5F) and increased NFATc1 protein levels in Jurkat T cells (online supplemental figure S5G). These results collectively support that TRIP12 lysine1136 tryptophanylation (Trp-K1136) activated its E3 activity toward NFATc1.

The levels of NFATc1 in HEK293T cells, but not in TRIP12^{K1136R} knockin HEK293T cells (online supplemental figure S5H), were reduced by tryptophan supplementation (figure 5D) or WARS overexpression (figure 5E), suggesting that Trp-K1136 is the major underlying mechanism connecting tryptophan and WARS to PD-1 expression. K1136 is located between the WWE and HECT domains of TRIP12 (online supplemental figure S5I). We, therefore, hypothesized that K1136Trp enhanced the ability of TRIP12 to degrade NFATc1 by enhancing the ability of TRIP12 to recruit NFATc1. Recombinant tryptophanylation-mimetic TRIP12, which switch lysine 1136 of TRIP12 into tryptophan (TRIP12^{K1136W}), had higher affinity than the WT TRIP12 to bind NFATc1 (figure 5F). Moreover, the affinity between TRIP12 and WARS was enhanced by Me-Trp supplementation (figure 5G), and the affinity between TRIP12 and NFATc1 was decreased by tryptophan deprivation (figure 5H), consistent with Me-Trp supplementation resulting in a dose-dependent increase in ubiquitination of NFATc1 (figure 5I), and tryptophan starvation leading to lower ubiquitination of NFATc1 (figure 5J). *WARS* knockdown decreased the affinity between TRIP12 and NFATc1 (figure 5K), and resulted in lower ubiquitination of NFATc1 (figure 5L). Conversely, WARS overexpression in HEK293T-*WARS*-KO cells increased the affinity between TRIP12 and NFATc1, but not between TRIP12^{K1136R} and NFATc1 (figure 5M), and resulted in higher ubiquitination of NFATc1 (figure 5N).

These results showed that K1136Trp positively regulated the E3 activity of TRIP12 toward NFATc1 by increasing TRIP12-NFATc1 interaction.

SIRT1 removed K1136Trp

We further investigated whether K1136Trp is dynamically regulated. NAD$^+$-dependent sirtuins (SIRTs), namely SIRT1-SIRT7,[34] can function as deaminoacylases.[19] Pansirtuin inhibitor NAM decreased the cell surface PD-1 and *PD-1* mRNA levels in anti-CD3 and anti-CD28 co-stimulated Jurkat T cells (figure 6A,B and online supplemental figure S6A. The cell surface PD-1 decreasing effects of NAM were recaptured in stimulated mouse CD8$^+$ T cells (figure 6C and online supplemental figure S6B). These results supported the possibility that K1136Trp is reversed by SIRTs. To pinpoint which SIRT possesses de-K1136Trp activity, we screened the abilities of SIRTs to reverse K1136Trp. When all SIRTs, namely SIRT1-7, were individually co-expressed with TRIP12 in HEK293T cells, SIRT1, SIRT6, and SIRT7 showed interaction with TRIP12 (figure 6D). However, only SIRT1 overexpression significantly decreased the tryptophanylation of isolated TRIP12 (figure 6E), and only SIRT1 overexpression clearly increased the surface PD-1 expression in Jurkat T cells (figure 6F and online supplemental figure S6C). These results suggested that SIRT1 is a de-tryptophanylase of K1136Trp. This notion was confirmed in SIRT1 KO C57BL/6 mice, in which decreased PD-1 expression in CD8$^+$ T cells was observed along with abrogated NAM ability to decreased surface PD-1 expression in CD8$^+$ T cells (figure 6G and online supplemental figure S6D, S6E). These results also suggest that SIRT1 is the major de-tryptophanylase of K1136Trp that regulates surface PD-1 expression.

Increase in tryptophanylation potentiated T cells to eliminate cancer cells

Tryptamine, an analog of tryptophan that competitively inhibits WARS,[33] reduced K1136Trp (online supplemental figure S5E) and induced the expression of cell surface PD-1 (figure 7A, online supplemental figure S7A) and *PD-1* mRNA (figure 7B) in Jurkat T cells and induced surface PD-1 expression in stimulated mouse CD8$^+$ T cells (figure 7C, online supplemental figure S7B), consistent with potentiation of T cells by tryptophanylation.

As CD8$^+$ T cells are the major effector cells in eliminating cancer cells,[35] we examined whether tryptophan treatment could increase the cytotoxic activity of CD8$^+$ T cells, since tryptophan (figure 1H) or IDO inhibitor (figure 2D) treatment decreased the expression of PD-1 in mouse CD8$^+$ T cells. CD8$^+$ T cells were isolated from OVA-stimulated mouse according to a previously reported protocol.[36] CD8$^+$ T cells were sorted from the OVA-immunized BALB/c splenocytes by surface CD3 and CD8 (online supplemental figure S7C and S7D). The ability of tryptophan to increase the toxicity of CD8$^+$ T cells was tested in LLC and mouse CT26 colorectal carcinoma cells. Tryptophan resulted in a dose-dependent increase in the
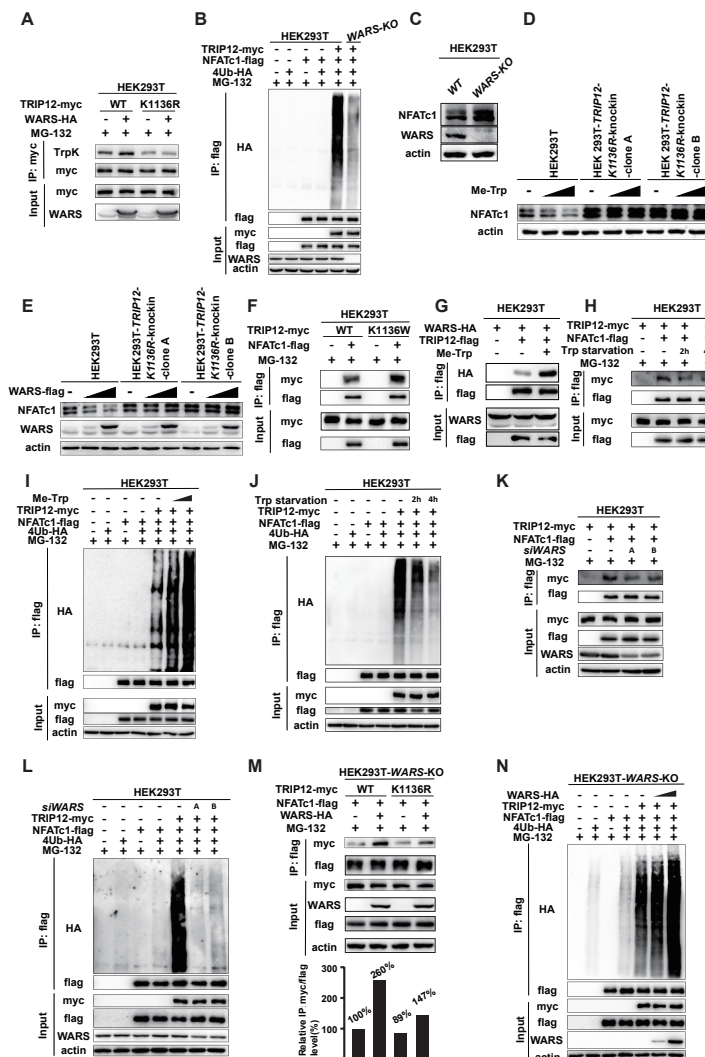
Figure 5 Tryptophanylation activates the E3 ligase activity of TRIP12. (A) Tryptophanyl-tRNA synthetase (WARS) increased TRIP12, but not TRIP12^{K1136R} tryptophanylation. Myc-tagged TRIP12 or TRIP12^{K1136R} was expressed alone or co-overexpressed with WARS-HA in HEK293T cells. The tryptophanylation levels of anti-myc beads purified TRIP12 and TRIP12^{K1136R} were examined. (B) *WARS* knockout decreased NFATc1 ubiquitination levels. NFATc1 was overexpressed alone or co-overexpressed with TRIP12 in WT or WARS-KO HEK293T cells. The ubiquitination levels of purified NFATc1 were detected. (C) *WARS* knockout increased endogenous NFATc1 levels. The NFATc1 levels in HEK293T cells and *WARS*-KO HEK293T cells were detected. Ablating TRIP12 tryptophanylation site abrogated Me-Trp supplemental or WARS overexpression to decrease NFATc1. NFATc1 levels were compared between HEK293T cells and TRIP12^{K1136R} knockin HEK293T cells that were subject to Me-Trp supplemental (D) or WARS overexpression (E). (F) Tryptophanylation mimetic TRIP12^{K1136W} had higher affinity to NFATc1 than wild-type TRIP12. Myc-tagged TRIP12 or TRIP12^{K1136W} was each co-overexpressed with NFATc1-flag in HEK293T cells. The amount of TRIP12 or TRIP12^{K1136W} that was co-immunoprecipitated with NFATc1 were detected. (G) Tryptophan altered the affinity between TRIP12 and WARS. FLAG-tagged TRIP12 was co-overexpressed with WARS-HA in HEK293T cells that were cultured with or without Me-Trp supplementation. The amount of WARS that was co-precipitated with TRIP12 was detected. (H) Tryptophan altered the affinity between TRIP12 and NFATc1. Flag-tagged NFATc1 was co-overexpressed with TRIP12-myc in HEK293T cells that were cultured with or without tryptophan starvation. The amount of TRIP12 that was co-precipitated with NFATc1 was detected. Tryptophan regulated the ubiquitination levels of NFATc1. NFATc1 was co-overexpressed with TRIP12 in HEK293T cells. The ubiquitination levels of NFATc1 from Me-Trp supplemented (I) and tryptophan starved (J) cells were compared with those of untreated cells. (K) *WARS* knockdown decreased the affinity between TRIP12 and NFATc1. Myc-tagged TRIP12 was co-overexpressed with NFATc1-Flag in HEK293T cells and in HEK293T cells with *WARS* knockdown. The amount of TRIP12 co-immunoprecipitated with NFATc1 was detected. (L) *WARS* knockdown decreased ubiquitination of NFATc1. NFATc1 was overexpressed alone or co-overexpressed with TRIP12 in HEK293T cells and in *WARS* knockdown HEK293T cells. The ubiquitination levels of purified NFATc1 were detected. (M) Tryptophanylation site ablation abrogated WARS to enhance TRIP12-NFATc1 interaction. The amount of Myc-tagged TRIP12 co-precipitated with NFATc1-flag was detected when they were co-overexpressed in *WARS*-KO HEK293T cells that were with or without WARS overexpression. Quantitation of the western blot analysis was shown. (N) WARS overexpression increased ubiquitination of NFATc1. NFATc1 was overexpressed alone or co-overexpressed with TRIP12 in *WARS*-KO HEK293T cells in the presence or absence of WARS overexpression. Ubiquitination levels of NFATc1 were compared.
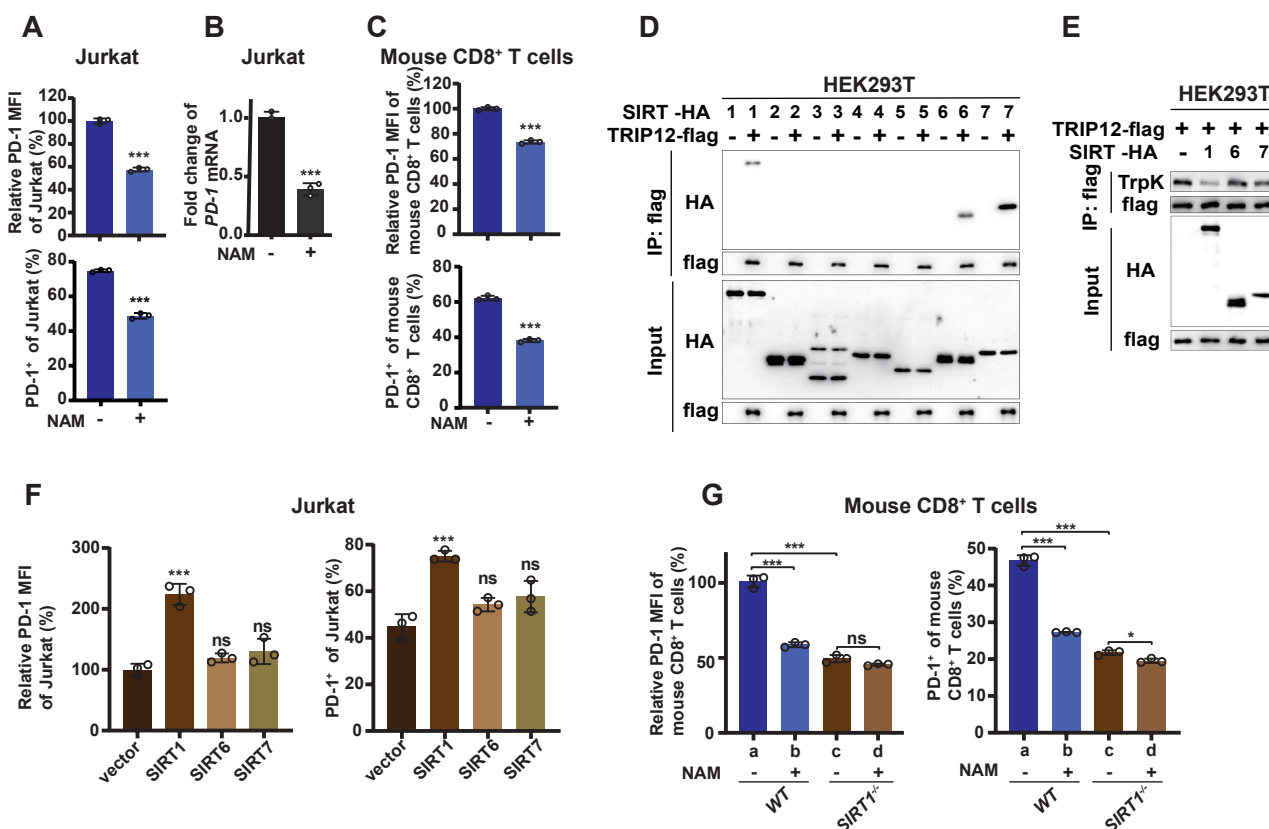
Figure 6 SIRT1 reverses TRIP12 K1136 tryptophanylation. Nicotinamide (NAM) decreased cell surface programmed cell death protein 1 (PD-1) and *PD-1* messenger RNA (mRNA) of Jurkat cells. Activated Jurkat T cells were treated with 5 mM NAM for 6 hours. PD-1 mean fluorescence intensity (MFI) and PD-1 positive cells were measured by flow cytometry (A). *PD-1* mRNA was examined by reverse transcription quantitative PCR (RT-qPCR) (B). (C) NAM decreased mouse CD8+ T cells surface PD-1. Naïve CD8+ T cells were isolated from the spleen of BALB/c wild-type (WT) mouse and stimulated with anti-CD3/CD28 antibodies. PD-1 MFI and PD-1 positive cells were compared between NAM-untreated and NAM-treated cells. (D) TRIP12-interacting SIRTs screening. HA-tagged SIRTs was individually co-expressed with TRIP12-flag in HEK293T cells. Interaction between TRIP12 and SIRTs was assayed by co-immunoprecipitation. (E) SIRT1 decreased the tryptophanylation of isolated TRIP12. HA-tagged SIRT1, SIRT2, SITR6, and SIRT7 were individually co-expressed with TRIP12-flag in HEK293T cells and the tryptophanylation levels of TRIP12 purified from each SIRT-expression cell were detected. (F) SIRT1 increased cell surface PD-1 expression. HA-tagged SIRT1, SIRT6, and SIRT7 were individually overexpressed in Jurkat T cells, relative PD-1 MFI and percentage of PD-1+ cells were measured. (G) *SIRT1* ablation in mice prevented NAM to decrease surface PD-1 expression. Naïve CD8+ T cells were isolated from the spleen of WT or *SIRT1*−/− C57BL/6 mice and activated. Relative PD-1 MFI and percentage of PD-1+ cells were compared between NAM-treated and NAM-untreated mouse CD8+ T cells. *P<0.05, ***p<0.001; ns, not significant.

apoptotic rate of LLC cells that were loaded with the OVA peptide (SIINFEKL) and co-cultured with CD8+ T cells at 1:10. Conversely, it had a negligible effect on the apoptotic rate of LLC that were cultured alone (figure 7D and online supplemental figure S7E). Enhancement in the toxicity of CD8+ T cells by tryptophan was also observed in mouse CT26 colorectal carcinoma cells (figure 7E and online supplemental figure S7F). These results, together with that kynurenine had negligible effects on TrpK and expression of NFATc1 (revised online supplemental figure S7G) and PD-1 (see figure 2C), IL-2, IFN-γ, and TNF-α (online supplemental figure S7H, I), showed that tryptophan potentiated the toxicity of CD8+ T cells by enhancing tryptophanylation toward cancer cells.

Consistent with the results of cultured cells, when LLC were injected subcutaneously into C57BL/6 mice, intraperitoneal administration of either Me-Trp or indoximod slowed down tumor growth and the combined treatment

of Me-Trp and indoximod resulted in synergistic effect on tumor growth inhibition (figure 7F,G). Two observations were made in tumor grafts following Me-Trp and indoximod treatments. First, both Me-Trp and indoximod decreased the PD-1 levels of the CD8+ T cells of mice spleens (figure 7H, online supplemental figure S7J) and tumor-infiltrating lymphocyte (TIL) CD8+ T cells, while combined treatment of Me-Trp and indoximod led to greater decrease of PD-1 (figure 7I, online supplemental figure S7K). Second, the number of CD4+ and CD8+ T cells in the tumor mass of Me-Trp-treated and indoximod-treated mice was more than double that of the tumors of untreated mice (figure 7J), Me-Trp and indoximod co-treatment showed a combined effect to enhance the number of CD4+ and CD8+ T cells, suggesting that these treatments enhanced CD8+ T cells survival and their tumor mass filtration ability.
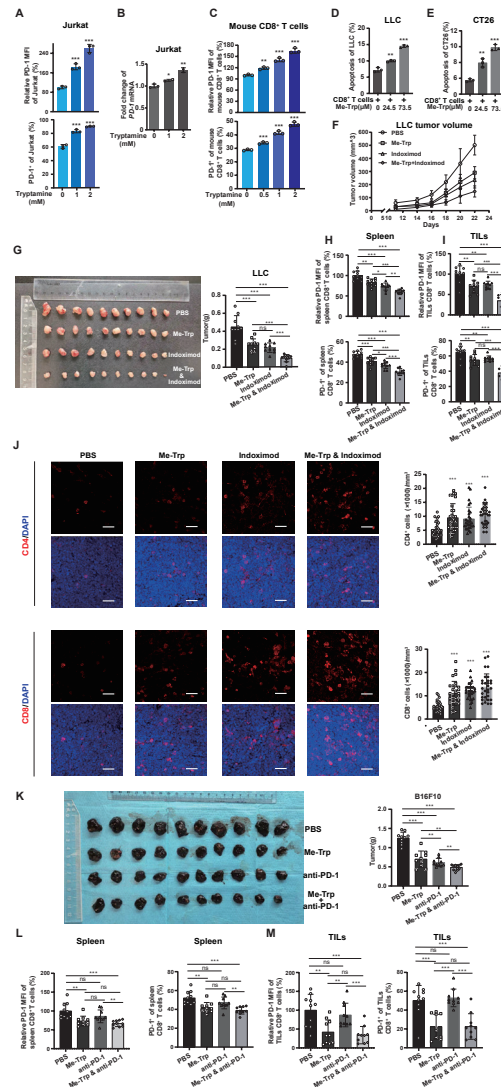
Figure 7 Increased tryptophanylation potentiates T cells to eliminate cancer cells. Tryptamine increased cell surface PD-1 and *PD-1* mRNA in Jurkat cells. Relative PD-1 MFI and percentage of PD-1+ cells (A) and *PD-1* mRNA (B) were measured in Jurkat T cells and tryptamine-treated Jurkat T cells. n=3, mean ± SD. (C) Tryptamine increased cell surface PD-1 in mouse CD8+ T cells. Naïve CD8+ T cells were isolated from the spleen of BALB/c WT mouse and activated with anti-CD3/CD28 antibodies. Relative PD-1 MFI and percentage of PD-1+ cells were measured in cells treated with tryptamine as indicated. n=3, mean±SD. Tryptophan dose-dependently increased the cytotoxicity of CD8+ T cells. CD8+ T cells were isolated from OVA-immuned BALB/c mice by flow cytometry.The apoptotic rate of LLC cells (D) and CT26 cells (E) that were co-cultured with CD8+ T cells (CD8+ T cell: LLC/CT26=10:1) in media contained different levels of Me-Trp were measured. n=3, mean±SD. Intraperitoneal dose of Trp and/or indoximod elicited regression of tumor growth. Mice inoculated with the same number of LLC cells were treated by intraperitoneal dose of Me-Trp or indoximod, both Me-Trp and indoximod, or PBS (control), the growth of tumors volume (F) and the tumor sizes and weights of sacrificed mice (G) were shown. n=10, mean±SD. Intraperitoneal dose of Trp and/or indoximod decreased the PD-1 levels. Spleen CD8+ T cells (H) and CD8+ T cells of tumor-infiltrating lymphocytes (TILs, I) were isolated from PBS, intraperitoneal dose of Me-Trp (Me-Trp), indoximod, and both Me-Trp and indoximod mice groups and analyzed on day 22. Relative MFI of surface PD-1 and percentage of PD-1+ cells were measured by flow cytometry. See also online supplemental Figure 7G-H for the sorting of CD8+ T cells. n=10, mean±SD. (J) Intraperitoneal dose of Trp or indoximod increased tumor-infiltrating CD8+ T cells. Confocal microscopy images of CD4 (red) or CD8 (red) staining on mouse tumor sections from PBS, intraperitoneal dose of Trp (Me-Trp), indoximod, and both Me-Trp and indoximod mice groups. DAPI (blue) showed the staining of nuclear. The density per volume of the CD4 or CD8-positive cells in the tumor sections corresponding to p value was calculated. Scale bar 50 μm, n=30 (three images randomly acquired from each mouse, and ten mice each group were included), mean±SD. (K) Intraperitoneal dose of Trp and/or anti-PD-1 elicited regression of tumor growth. Mice inoculated with B16F10 cells were treated by intraperitoneal dose of Me-Trp or anti-PD-1, both Me-Trp and anti-PD-1, or PBS (control), the tumor sizes and weights of sacrificed mice were shown. n=10, mean±SD. Intraperitoneal dose of Trp or Trp combining anti-PD-1 decreased the PD-1 levels. Spleen CD8+ T cells (L) and CD8+ T cells of tumor-infiltrating lymphocytes (TILs, M) were isolated from PBS, intraperitoneal dose of Me-Trp (Me-Trp), anti-PD-1, and Me-Trp and anti-PD-1 combined mice groups and analyzed on day 14. Relative MFI of surface PD-1 and percentage of PD-1+ cells were measured by flow cytometry. n=10, mean±SD.

To generalize the tumor growth inhibition effects of tryptophanylation by downregulating PD-1 and activating T cells, we examined tryptophan-supplemental effects on tumor growth of B16F10 melanoma cells under with and without PD-1 antibody injection. Tryptophan decreased the growth of B16F10 tumor cells (figure 7K) and decreased surface PD-1 levels in both spleen and TIL CD8^{+} T cells (figure 7L,M), suggested that tryptophan supplemental inhibits growth of cancer cells regardless of their origins. Moreover, although both tryptophan and PD-1 antibody caused tumor regression, tryptophan exerted a potency to inhibit tumor growth in mice treated with PD-1 antibody (figure 7K-M). The synergistic effects of PD-1 antibody and tryptophan supported that tryptophan exerts its antitumor effects through inhibiting PD-1.

DISCUSSION

The unveiling of protein aminoacylation[19] has opened new angles for investigating the biological processes and regulatory roles of amino acids. The immune cell suppression by tryptophan has been often attributed to T cell suppression by tryptophan catabolites. In the current study, we provided evidence at various levels to show that tryptophan accumulation may also account for IDO inhibitors' immunity boosting efficacies because tryptophan is a T cell activator. Tryptophan activates T cells by downregulating their inhibitory protein PD-1 expression via the WARS-TRIP12-NFATc1-*PD-1* axis. WARS tryptophanylates and activates TRIP12, an E3 ligase of the transcription factor NFATc1 that positively regulates *PD-1* expression to activate T cells, and tryptophan-activated T cells can be inhibited by SIRT1, which de-tryptophanylates Trp-K1136 and reverses consequences of TRIP12 tryptophanylation. These results unveiled that tryptophan activates T cells through lysine tryptophanylation, while its catabolites inhibit T cells via other mechanisms (online supplemental figure S8). Therefore, IDO suppresses immunity by producing tryptophan catabolites and by decreasing tryptophan levels and IDO inhibitors activate immunity by reversing these two consequences.

Mounting documented studies supported our findings. Tryptophan levels are positively associated with immunity, as IFN-γ-enhanced tryptophan catabolism to deplete tryptophan exerts immune repression, although this efficacy was mainly explained by the fact that increases of the levels of tryptophan catabolites, such as quinolinic acid and 3-hydroxyanthranilic acid, can inhibit the proliferation of immune cells and promote their apoptosis.[14 37–42] WARS levels are positively correlated with T cell activation and are consistent with our model. CD8^{+} T cells with increased WARS expression are able to maintain their activation status.[43 44] In immune thrombocytopenia, decreased IDO expression and increased WARS expression in CD4^{+} and CD8^{+} cells have been proposed to enhance the survival of autoreactive T cells.[45] Consistent with such hypothesis, cancer cells overexpress IDO[6] to create a microenvironment that has both decreased tryptophan and increased tryptophan catabolites to avoid activation of T cells. In patients with rheumatoid arthritis, the increased expression of *WARS* mRNA may be a cause of CD3^{+} T cell activation.[46] In several cancers, including gastric adenocarcinoma, and colorectal and ovarian cancers, high levels of WARS expression are associated with a favorable prognosis,[47–49] likely due to the fact that WARS is a secretable protein which is rapidly secreted in response to viral infection,[50] and elevated circulating WARS may increase tryptophanylation levels and activate T cells, favoring tumor immune elimination. Furthermore, SIRT1 inhibitor sirtinol treatment in infected mice decreased their spleen parasite burden, and PD-1 inhibitor showed a synergistic effect,[51] supporting that SIRT1 inhibition would phenocopy tryptophan and IDO inhibitor to activate immunity. All these observations may be explained by the activation of T cells by tryptophanylation as proposed and demonstrated in this study, although they were initially explained by various mechanisms.

Both physiological tryptophan and its catabolites are low, with tryptophan at 10–100 µM and kynurenine at 5–50 µM.[12] Therefore, although IDO inhibitors can increase tryptophan and decrease tryptophan catabolites, both result in T cells activation, their clinical anticancer efficacies are suboptimal, likely due to that IDO inhibitors can hardly vary levels of tryptophan and tryptophan catabolites to extent big enough to exert sufficient immunity-boosting power. We showed that Me-Trp supplemental increased intracellular tryptophan levels and tryptophan catabolites, and activated CD8^{+} T cells, suggesting that the opposite effects of tryptophan and its catabolites are dependent on the relative intracellular concentrations. This can be explored in IDO inhibitor cancer therapy. Tryptophan supplemental in combination with IDO inhibitor, which may greatly increase intracellular tryptophan levels while keeping tryptophan catabolites at low levels, had much stronger ability to prevent cancer growth. Moreover, because tryptophan activates T cells by decreasing PD-1 expression, a combination of tryptophan, IDO inhibitors, and PD-1 antibodies would be expected even more powerful strategy to fight against cancer.

Author affiliations
[1]State Key Laboratory of Genetic Engineering, School of Life Sciences and Obstetrics & Gynecology Hospital of Fudan University, Shanghai, China
[2]NHC Key Lab of Reproduction Regulation (Shanghai Institute of Planned Parenthood Research), Shanghai Key Laboratory of Metabolic Remodeling, Institute of Metabolism and Integrative Biology and Institutes of Biomedical Sciences, Shanghai, China
[3]Department of Cardiology, Children's Hospital of Fudan University, Shanghai, China
[4]Key Laboratory for Tibet Plateau Phytochemistry of Qinghai Province, College of Pharmacy, Qinghai University for Nationalities, Xining, China

Competing interests No, there are no competing interests.

Patient consent for publication Not required.

Ethics approval All animal experiments were carried out in full accordance with animal ethic regulations of Fudan University, Shanghai, China.

Provenance and peer review Not commissioned; externally peer reviewed.

Data availability statement Data are available on reasonable request. All data relevant to the study are included in the article or uploaded as supplementary information.

ORCID iD
Shimin Zhao http://orcid.org/0000-0002-3674-9107

REFERENCES

1. Wang X, He Q, Shen H, *et al*. TOX promotes the exhaustion of antitumor CD8^{+} T cells by preventing PD1 degradation in hepatocellular carcinoma. *J Hepatol* 2019;71:731–41.
2. Okamura H, Okazaki I-M, Shimizu K, *et al*. PD-1 aborts the activation trajectory of autoreactive CD8^{+} T cells to prohibit their acquisition of effector functions. *J Autoimmun* 2019;105:102296.
3. Maleki Vareki S, Garrigós C, Duran I. Biomarkers of response to PD-1/PD-L1 inhibition. *Crit Rev Oncol Hematol* 2017;116:116–24.
4. Araki K, Youngblood B, Ahmed R. Programmed cell death 1-directed immunotherapy for enhancing T-cell function. *Cold Spring Harb Symp Quant Biol* 2013;78:239–47.
5. Uyttenhove C, Pilotte L, Théate I, *et al*. Evidence for a tumoral immune resistance mechanism based on tryptophan degradation by indoleamine 2,3-dioxygenase. *Nat Med* 2003;9:1269–74.
6. Löb S, Königsrainer A, Zieker D, *et al*. Ido1 and IDO2 are expressed in human tumors: levo- but not dextro-1-methyl tryptophan inhibits tryptophan catabolism. *Cancer Immunol Immunother* 2009;58:153–7.
7. Munn DH, Zhou M, Attwood JT, *et al*. Prevention of allogeneic fetal rejection by tryptophan catabolism. *Science* 1998;281:1191–3.
8. Löb S, Königsrainer A, Rammensee H-G, *et al*. Inhibitors of indoleamine-2,3-dioxygenase for cancer therapy: can we see the wood for the trees? *Nat Rev Cancer* 2009;9:445–52.
9. Zhu MMT, Dancsok AR, Nielsen TO. Indoleamine dioxygenase inhibitors: clinical rationale and current development. *Curr Oncol Rep* 2019;21:2.
10. Vacchelli E, Aranda F, Eggermont A, *et al*. Trial Watch: IDO inhibitors in cancer therapy. *Oncoimmunology* 2014;3:e957994.
11. Dai W, Gupta SL. Regulation of indoleamine 2,3-dioxygenase gene expression in human fibroblasts by interferon-gamma. upstream control region discriminates between interferon-gamma and interferon-alpha. *J Biol Chem* 1990;265:19871–7.
12. Fallarino F, Grohmann U, Vacca C, *et al*. T cell apoptosis by tryptophan catabolism. *Cell Death Differ* 2002;9:1069–77.
13. Munn DH, Sharma MD, Baban B, *et al*. Gcn2 kinase in T cells mediates proliferative arrest and anergy induction in response to indoleamine 2,3-dioxygenase. *Immunity* 2005;22:633–42.
14. Munn DH, Shafizadeh E, Attwood JT, *et al*. Inhibition of T cell proliferation by macrophage tryptophan catabolism. *J Exp Med* 1999;189:1363–72.
15. Holmgaard RB, Zamarin D, Munn DH, *et al*. Indoleamine 2,3-dioxygenase is a critical resistance mechanism in antitumor T cell immunotherapy targeting CTLA-4. *J Exp Med* 2013;210:1389–402.
16. Botticelli A, Cerbelli B, Lionetto L, *et al*. Can IDO activity predict primary resistance to anti-PD-1 treatment in NSCLC? *J Transl Med* 2018;16:219.
17. Ladomersky E, Zhai L, Lauing KL, *et al*. Advanced age increases immunosuppression in the brain and decreases immunotherapeutic efficacy in subjects with glioblastoma. *Clin Cancer Res* 2020;26:5232–45.
18. Agata Y, Kawasaki A, Nishimura H, *et al*. Expression of the PD-1 antigen on the surface of stimulated mouse T and B lymphocytes. *Int Immunol* 1996;8:765–72.
19. He X-D, Gong W, Zhang J-N, *et al*. Sensing and transmitting intracellular amino acid signals through reversible lysine aminoacylations. *Cell Metab* 2018;27:151–66.
20. Park SG, Schimmel P, Kim S. Aminoacyl tRNA synthetases and their connections to disease. *Proc Natl Acad Sci U S A* 2008;105:11043–9.
21. Moellering RE, Cravatt BF. Functional lysine modification by an intrinsically reactive primary glycolytic metabolite. *Science* 2013;341:549–53.
22. Vidal C, Li W, Santner-Nanan B, *et al*. The kynurenine pathway of tryptophan degradation is activated during osteoblastogenesis. *Stem Cells* 2015;33:111–21.
23. Huang Q, JJ X, Wang L. miR-153 suppresses IDO1 expression and enhances CAR T cell immunotherapy (Vol 11, 58, 2018). *Journal of Hematology & Oncology* 2018;11.
24. Liu X-Q, Lu K, Feng L-L, *et al*. Up-Regulated expression of indoleamine 2,3-dioxygenase 1 in non-Hodgkin lymphoma correlates with increased regulatory T-cell infiltration. *Leuk Lymphoma* 2014;55:405–14.
25. Ishida Y, Agata Y, Shibahara K, *et al*. Induced expression of PD-1, a novel member of the immunoglobulin gene superfamily, upon programmed cell death. *Embo J* 1992;11:3887–95.
26. Metz R, Rust S, Duhadaway JB, *et al*. Ido inhibits a tryptophan sufficiency signal that stimulates mTOR: a novel IDO effector pathway targeted by D-1-methyl-tryptophan. *Oncoimmunology* 2012;1:1460–8.
27. Cho J-H, Kim H-O, Kim K-S, *et al*. Unique features of naive CD8+ T cell activation by IL-2. *J Immunol* 2013;191:5559–73.
28. Xia H, Jiang W, Zhang X, *et al*. Elevated Level of CD4^{+} T Cell Immune Activation in Acutely HIV-1-Infected Stage Associates With Increased IL-2 Production and Cycling Expression, and Subsequent CD4^{+} T Cell Preservation. *Front Immunol* 2018;9:616.
29. Oestreich KJ, Yoon H, Ahmed R, *et al*. Nfatc1 regulates PD-1 expression upon T cell activation. *J Immunol* 2008;181:4832–9.
30. Aramburu J, Yaffe MB, López-Rodríguez C, *et al*. Affinity-driven peptide selection of an NFAT inhibitor more selective than cyclosporin A. *Science* 1999;285:2129–33.
31. Lefebvre AM, Chen I, Desreumaux P, *et al*. Activation of the peroxisome proliferator-activated receptor gamma promotes the development of colon tumors in C57BL/6J-APCMin/+ mice. *Nat Med* 1998;4:1053–7.
32. Schramme F, Crosignani S, Frederix K, *et al*. Inhibition of Tryptophan-Dioxygenase activity increases the antitumor efficacy of immune checkpoint inhibitors. *Cancer Immunol Res* 2020;8:32–45.
33. Paley EL, Denisova G, Sokolova O, *et al*. Tryptamine induces tryptophanyl-tRNA synthetase-mediated neurodegeneration with neurofibrillary tangles in human cell and mouse models. *Neuromolecular Med* 2007;9:55–82.
34. Anderson KA, Green MF, Huynh FK, *et al*. Snapshot: mammalian sirtuins. *Cell* 2014;159:956–956.e1.
35. Durgeau A, Virk Y, Corgnac S, *et al*. Recent advances in targeting CD8 T-cell immunity for more effective cancer immunotherapy. *Front Immunol* 2018;9:14.
36. Ou-Yang C-wen, Zhu M, Fuller DM, *et al*. Role of LAT in the granule-mediated cytotoxicity of CD8 T cells. *Mol Cell Biol* 2012;32:2674–84.
37. Munn DH, Mellor AL. Ido in the tumor microenvironment: inflammation, counter-regulation, and tolerance. *Trends Immunol* 2016;37:193–207.
38. Wang X-F, Wang H-S, Wang H, *et al*. The role of indoleamine 2,3-dioxygenase (IDO) in immune tolerance: focus on macrophage polarization of THP-1 cells. *Cell Immunol* 2014;289:42–8.
39. Soliman H, Mediavilla-Varela M, Antonia S. Indoleamine 2,3-dioxygenase: is it an immune suppressor? *Cancer J* 2010;16:354–9.
40. Mellor AL, Munn DH. Ido expression by dendritic cells: tolerance and tryptophan catabolism. *Nat Rev Immunol* 2004;4:762–74.
41. Grohmann U, Fallarino F, Puccetti P. Tolerance, DCs and tryptophan: much ado about IDO. *Trends Immunol* 2003;24:242–8.
42. Munn DH, Sharma MD, Lee JR, *et al*. Potential regulatory function of human dendritic cells expressing indoleamine 2,3-dioxygenase. *Science* 2002;297:1867–70.
43. Boasso A, Herbeuval J-P, Hardy AW, *et al*. Regulation of indoleamine 2,3-dioxygenase and tryptophanyl-tRNA-synthetase by CTLA-4-Fc in human CD4+ T cells. *Blood* 2005;105:1574–81.
44. Finger EB, Bluestone JA. When ligand becomes receptor--tolerance via B7 signaling on DCs. *Nat Immunol* 2002;3:1056–7.

45 Wang C-Y, Shi Y, Min Y-N, *et al*. Decreased IDO activity and increased TTS expression break immune tolerance in patients with immune thrombocytopenia. *J Clin Immunol* 2011;31:643–9.

46 Chen J, Jun L, Shiyong C, *et al*. Increased TTS expression in patients with rheumatoid arthritis. *Clin Exp Med* 2015;15:25–30.

47 Ghanipour A, Jirström K, Pontén F, *et al*. The prognostic significance of tryptophanyl-tRNA synthetase in colorectal cancer. *Cancer Epidemiol Biomarkers Prev* 2009;18:2949–56.

48 Patil PA, Blakely AM, Lombardo KA, *et al*. Expression of PD-L1, indoleamine 2,3-dioxygenase and the immune microenvironment in gastric adenocarcinoma. *Histopathology* 2018;73:124–36.

49 Cheong J-H, Yang H-K, Kim H, *et al*. Predictive test for chemotherapy response in resectable gastric cancer: a multi-cohort, retrospective analysis. *Lancet Oncol* 2018;19:629–38.

50 Ahn YH, Park S, Choi JJ, *et al*. Secreted tryptophanyl-tRNA synthetase as a primary defence system against infection. *Nat Microbiol* 2016;2:16191.

51 Roy S, Saha S, Gupta P, *et al*. Crosstalk of PD-1 signaling with the SIRT1/FOXO-1 axis during the progression of visceral leishmaniasis. *J Cell Sci* 2019;132. doi:10.1242/jcs.226274. [Epub ahead of print: 02 05 2019].